STATISTICS OF BENDING MOMENT IN THE SPLASH ZONE OF A TENSIONED RISER

Xiao Gan

MASTER THESIS SPRING 2014

for

Stud.tech. Xiao Gan

STATISTICS OF BENDING MOMENT IN THE SPLASH ZONE OF A TENSIONED RISER

(Statistiske egenskaper for bøyemoment i et stigerør i bølgesonen)

For marine drilling risers, in order to stand the damage in design lifetime, the ultimate limit state is of interest. In order to perform assessment for ultimate limit state, the extreme response of the riser should be fully understood. Wave forces on marine risers are normally calculated by use of Morison's equation. This model is simple to use and accepted as adequate for this purpose. The model is hence used to calculate local forces for vertical risers in the wave zone. The main problem with this application is that the response will have strong nonlinear nature, which makes the post-process of the response distribution more difficult. Rayleigh distribution cannot be used to describe the riser response distribution anymore. Thus an alternative method should be investigated for nonlinear response. The full long-term dynamic analysis can be used for this purpose, in addition it can give a relatively accurate result. However, it is time-consuming and complicated for strong nonlinear system. A simplified method is normally used to perform short-term analysis instead of full long-term analysis to simplify the simulation process.

The statistical uncertainty for estimates based on time records of limited duration will then become important. This type of uncertainty can in principle be reduced by increasing the length of the time record used for estimation, but the relevance of using very long records is questionable since the model uncertainty still we be important. A consistent approach to both types of uncertainty must therefore be taken. The purpose of the present project is to investigate both uncertainties and propose a procedure for stochastic analysis that gives a reasonable balance of uncertainties.

The work should be organized in subtasks as follows:

1. Literature study, which should include material related to wave theory, Morison's equation, simplified long-term statistic method and stochastic analysis.
2. Use the computer program Riflex to carry out stochastic analyses of a tensioned riser in order to obtain necessary time history of response for simplified long-term statistic method.
3. Define the whole post-process method, find out the most suitable distribution for response fitting.
4. Find out the uncertainties of the simulation and discuss.

The work may show to be more extensive than anticipated. Some topics may therefore be left out after discussion with the supervisor without any negative influence on the grading.

The candidate should in her/his report give a personal contribution to the solution of the problem formulated in this text. All assumptions and conclusions must be supported by mathematical models and/or references to physical effects in a logical manner. The candidate should apply all available sources to find relevant literature and information on the actual problem.

The report should be well organised and give a clear presentation of the work and all conclusions. It is important that the text is well written and that tables and figures are used to sup-port the verbal presentation. The report should be complete, but still as short as possible.

The final report must contain this text, an acknowledgement, summary, main body, conclusions and suggestions for further work, symbol list, references and appendices. All figures, tables and equations must be identified by numbers. References should be given by author name and year in the text, and presented alphabetically by name in the reference list. The re-port must be submitted in two copies unless otherwise has been agreed with the supervisor.

The supervisor may require that the candidate should give a written plan that describes the progress of the work after having received this text. The plan may contain a table of content for the report and also assumed use of computer resources. From the report it should be possible to identify the work carried out by the candidate and what has been found in the available literature. It is important to give references to the original source for theories and experimental results. The report must be signed by the candidate, include this text, appear as a paperback, and - if needed - have a separate enclosure (binder, DVD/ CD or memory stick) with additional material.

Deadline: 10 June 2014

Carl M. Larsen
Supervisor

Acknowledge

Summary

Marine drilling riser extends from the drilling platform to the sea bottom, it experiences loads and motions from the environment and the vessel such as wave and current. In order to avoid the ultimate state failure, extreme loads should be correctly simulated. This is the main purpose of this thesis, to find out the extreme bending moment for a tensioned top riser at design lifetime.

For simplicity and practical purpose, hydrodynamic loads in tensioned riser are calculated by Morison's equation with acceptable accuracy in engineering in the wave zone. As it is know that the responses of tensioned riser are non-Gaussian due to the nonlinearities introduced by the hydrodynamic loading. For nonliear system, full long-term dynamic analysis can provide a relatively accurate result. However, it is almost impossible for complicated systems, since it is so time-consuming for computers even nowadays. Hence simplified long-term statistic (SLTS) method proposed by professor Larsen is studied in this work to simplify the extreme estimation of slender structure.

The main idea of SLTS method is to find a design storm that the extreme responses of a structure in its design lifetime can be obtained from this seastate, instead of performing full long-term time-domain dynamic analysis. The design storm is found in an approximate long-term response analysis, establish by the results from frequency domain analysis. However, the computer simulation program *SIMA* does not include a frequency domain solver, the frequency domain simulation is replaced by time domain simulation. Short time simulation of each selected seastate is performed in time domain in order to find the zero up-crossing period and variance, which can be used to establish approximate short-term distribution for each seastate. The distributions are described by Rayleigh distribution. From approximate short-term distributions, an approximate long-term distribution can be established, thus the approximate response amplitude and seastate with largest short-term probability can be identified. This is design storm. The estimation of maximum bending moment can thus perform only in a short-term simulation, since the design storm is expected to cause the maximum bending moment in lifetime.

In order to find a more correct statistical property, an 8-hour simulation was performed for design storm. The easiest way to reduce simulation uncertainty is to perform long time simulation. 9 random phase angles are used to generate irregular waves, and time history of response from all the phase angles are provided from time domain dynamic analysis in *SIMA*.

Time history of response could not tell us which response is the possible extreme response, hence post-process of time history data is needed. The main idea is to build up a distribution with data taken from time history to predict the response amplitude

under certain probability of exceedance. In this work, the probability of exceedance is taken from the approximate short-term probability of design seastate. For non-Gaussian process, Rayleigh distribution is not suitable. Both two- and three-parameter Weibull distribution were tested, it proved that only the application of three-parameter Weibull distribution on the upper tail of the response distribution can give a satisfactory fitting. Then the maximum bending moment can be read out from the corresponding probability of exceedance.

Simulation uncertainty is an important factor that influence the accuracy of the extreme response estimation. In this thesis, uncertainties such as simulation length, number of data in tail function and phase angels were studied. It can be concluded that the phase angels give a significant uncertainty to the simulation. The deviation of extreme responses from different phase angle of irregular wave can be up to 11%.

Nomenclature

NTNU   Norwegian University of Science and Technology

SLTS   Simplified Long-Term Statistic

DP   Dynamic Positioning

BOP   Blow-out Preventer

LMRP   Lower Marine Riser Package

NPV   Nitrogen Pressure Vessels

FFT   Fast Fourier Transformation

FE   Finite Element

FEM   Finite Element Method

DAF   Dynamic Amplification Factor

RAO   Response Amplitude Operator

Contents

List of Figures

List of Tables

Chapter 1

Introduction

1.1 Motivation

Marine tensioned riser is an important part of marine drilling system. It is exposed to a variety of loads, including hydrodynamic loads from wave and current, and the top-end vessel motion. Thus it has a risk of environmental damage, structure failure or damage to the material. The design of marine tensioned riser must satisfy the ultimate, fatigue and accidental limit state, in order to stand the damage in design lifetime. In this thesis, the ultimate limit state is of most interest, thus the extreme response of the riser should be fully understood. This thesis will concentrate on methods to estimate the extreme response, to be specified, extreme bending moment in lifetime.

Before simulating the marine riser behaviour, the sea environment should be modelled in a random nature. The sea environment can be described in terms of environmental parameters, such as wave height, period, direction and length, which is called seastate. For practical purpose the wave process can be assumed as a stationary process in a short time period. however, in order to describe the random and irregular sea environment, scatter diagrams are widely used to describe the long-term variation of wave climate for governing seastate parameters. A scatter diagram provides the frequency of occurrence of a given parameter, and conditional or marginal distribution of the seastate parameter can also be obtained[8]. Wave spectra is usually used to determine the energy distribution of a given seastate, in terms of the wave frequency. Which means that the sea condition of given seastate is built up by the waves with different frequencies. In this way, the loads condition can be calculated in a given seastate.

Irregular wave generation is an important factor to the uncertainty of simulation, the generation method will be discussed in detail in Chapter 3.

For simplicity, hydrodynamic loads in slender structures are normally calculated by Morison equation with acceptable accuracy in engineering. Thus this method can be used to calculate local forces for vertical risers in the wave zone. However, problem arises as linear wave theory cannot define fluid motions in a wave crest in a consistent way. Methods have to be proposed to calculate wave induced velocities and accelerations. Various methods have been proposed as engineering type of approximation, such as Wheeler stretching and relocation of the potential from mean water level to the actual wave surface. Since they are estimation to the fluid motions on the wave crest, uncertainty exists. It will be

discussed in chapter 4.

The ultimate limit state is defined as the collapse of the structure, which means the loss of its ability to withstand loads[9]. For slender structure like marine risers with strong dynamic effects, the response will have nonlinear nature. Because of the nonlinear effect, time-domain dynamic analysis will be applied to find the response in each set time step. The main target of this thesis is to study the statistical method used to deal with a large amount of data points in time history.

In practice, at least three methods statistical design method are available for marine riser: design storm, environmental contour line method and long-term response statistics. Design storm method will be used in this thesis, the rest will be introduced.

In time domain analysis, the uncertainty can be reduced by increasing the time duration for estimation. However, the length of time record cannot be infinitely long, the uncertainty should be investigated. The uncertainty of simulations will be an important part to study.

1.2 Previous Work

In the early 1990, Professor Carl Martin Larsen etc. proposed a new strategy for estimation of extreme response in tensioned marine risers. It was outlined and discussed in relation to more conventional methods such as regular wave, design storm and direct use of long-term response statistics[10]. This thesis will be based on this method, and more uncertainty effects will be studied.

1.3 Scope of Work

The overall purpose of this thesis is to study the whole theory of estimating the extreme response of marine risers, from generating wave to statistics of response. In order to understand the nonlinear nature of riser response, SLTS method will be applied to the dynamic analysis of tensioned riser. Long time simulation will be needed for a proper statistical description. The simulation will be performed in program *SIMA* developed by Marintek etc.. There are limits in the statistical method, thus uncertainty study is also of importance. The flow chart of the whole stochastic dynamic analysis method are presented in Figure 1.1. The content of this thesis will follow the flow chart sequence.

Chapter 2 introduces the marine drilling system, including the marine drilling riser components, heave compensation system. Characteristics and modelling method of the riser in *SIMA* was mentioned as well.

Chapter 3 discusses the generating method of irregular wave. In addition, statistics of waves, consisted of short-term and long-term distribution of wave, were introduced.

Chapter 4 mainly describes the Morison Equation, which is used to calculate the hydrodynamic loads in slender structure. In order to calculate the wave kinematics in the wave crest, modification of Airy wave theory was discussed.

Chapter 5 illustrates the finite element method used for dynamic analysis, combined with the finite element model in *SIMA*. Both static and dynamic methods are introduced, including the frequency domain and time domain analysis in dynamic method.

Chapter 6 introduces the statistics of response, consisting stochastic long-term and short-term response analysis.

Chapter 7 is the most main part of this thesis. It illustrates the whole procedure of application of SLTS method.

Chapter 8 is the discussion of the results from Chapter 7.

Chapter 9 concludes the final results and contribution of the whole thesis.

Statistics of Waves

↓

Calculation of
Hydrodynamic Loads

↓

Dynamics Response
Analysis

↓

Statistics of Response

↓

Design According to Rule
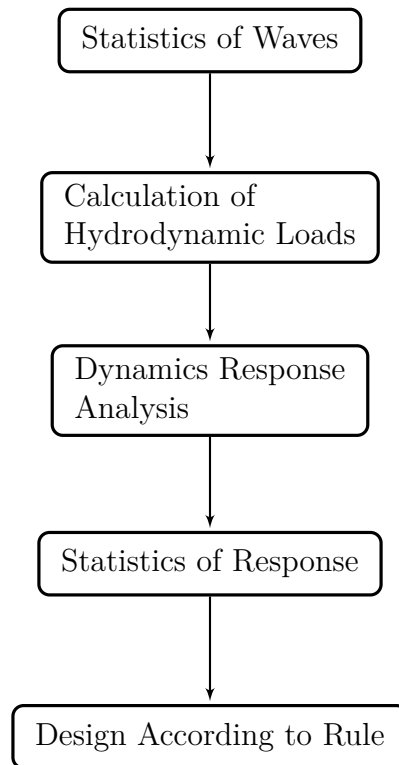
Figure 1.1: Stochastic Analysis of Marine Structures

Chapter 2

Marine Drilling Riser System

2.1   Marine Drilling Riser

Marine risers were fist used to drill from barges offshore California in the 1950s. In 1961 an important landmark occurred when drilling took place from the DP barge CUSS-1. Since those early days, risers have been used for four main purposes.

- Drilling

- Completion/workover

- Production/injection

- Export

In each of the four groups of risers there is a large variety of details, dimensions and materials. In this thesis we will only focus on drilling risers. The drilling risers are used for drilling wells in the sea bed, which are used on drilling semisubmersibles and drilling ships as shown in Figure 2.1. DP system is used to maintain their position under operation.

Drilling riser can be divided into low-pressure and high-pressure risers[11]. Nowadays, low-pressure riser is the most commonly used drilling riser. Low-pressure riser means the only internal pressure is that from the weight of the drilling-mud weight, which is open to the atmospheric pressure in the top end. Drilling risers are made up of joints, called strings, which can typically vary between 15-23 meters in length. They are tied together on each end to extend from the floater to the sea bed. The joints consist of a tubular midsection with riser connectors in the ends. As we can see from Figure 2.2, the main body of a drilling riser is comprised of a drilling string, a central tube, auxiliary lines and kill and choke lines. The nominal diameter of the central tube is usually 21 inches. Outside the central tube, the kill and choke lines are attached, in order to control the blow-out preventer (BOP) and fluid flow. If a BOP is closed due to a kick in the well, kill and choke lines are used to communicate with the well and to circulate fluid. The two auxiliary lines shown in Figure2.2 can be hydraulic lines, which are used to power the subsea BOP.

In addition, some key components of typical drilling riser system are shown in Figure 2.3[1].
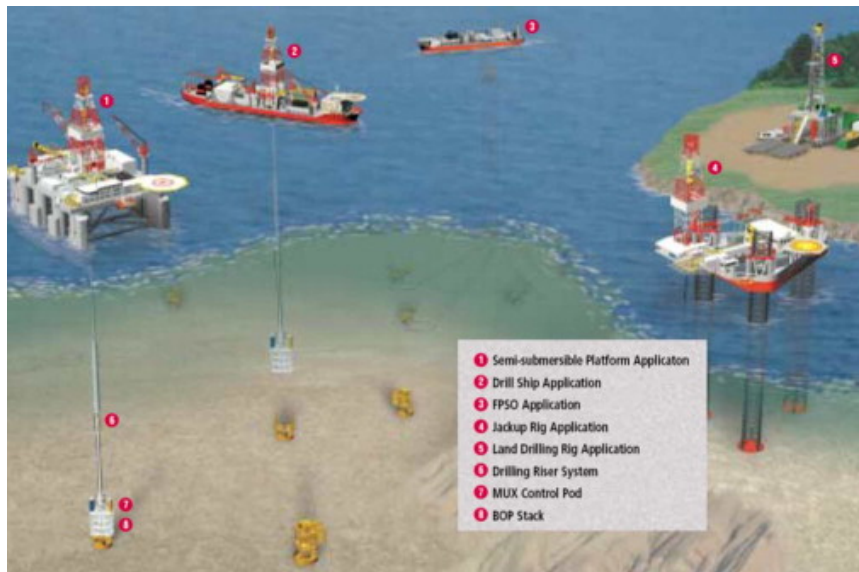
Figure 2.1: Drilling Semisubmersibles, Drilling Ships, and Drilling Risers [1]

Figure 2.2: Drilling risers with buoyancy modules to the left - 3D figure of the riser, drill string and kill/choke/auxiliary lines to the right [2]

- **Spider**. The spider is a device with retractable jaws or dogs used to hold and support the riser on the upper most connector support shoulder during running of the riser. The spider usually sits in the rotary table on the drill floor.

- **Gimbal**. The gimbal is installed between the spider and the rotary table. It is used to reduce shock and to evenly distribute loads caused by a rig's roll/pitch motions, on the spider as well as the riser sections.

- **Telescope joint**. A slick joint, also known as a telescope joint, consists of two concentric pipes that telescope together. It is a special riser joint designed to prevent damage to the riser and control umbilicals where they pass through the rotary table. Further more, it protects the riser from damage due to rig heave.

The joints shown in Figure 2.2 are equipped with syntactic foam buoyancy modules, in order to reduce the weight of the riser in water. The upper part the the riser's length is always equipped with such modules. In the lower part of the riser, because the density
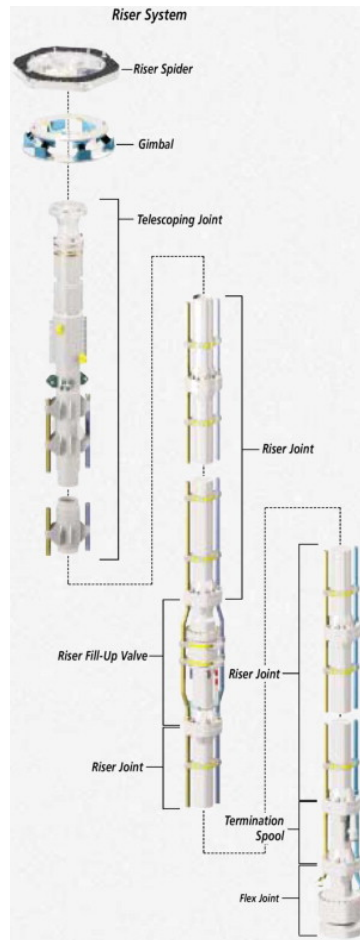
Figure 2.3: Key components in Drilling Riser System

and cost of the syntactic foam increase with depth and pressure, it is usually left bare. At a short distance near the surface, the riser is always left bare, for the purpose of reducing hydrodynamic force where wave forces are the highest[3].

Figure 2.4 a) and b) show drilling riser below a drilling ship and a semisubmersible. Two important riser components are shown in the figure, which are BOP and Lower Marine Riser Package (LMRP). In case of emergency, BOP will close the well and the drill string can be cut. Then the LMRP allows the riser to be disconnected.Between the riser and the LMRP there is a flex joint to bear limited rotation from the riser and to avoid concentrated moments.

2.2 Heave compensation system

Drilling risers are a completely vertical riser system that terminates directly below the facility. Although these floating facilities are moored, they are able to move along wind and waves. Since the rigid risers are fixed to the sea floor, vertical displacement occurs between the top of the riser and its connection point on the facility. Also since the bending stiffness of a long riser is low,top tension must be introduced to carry the weight of the riser, and to provide lateral stiffness needed to limit deflections due to wave and current forces. There are two solutions for this issue. A motion compensator can be included
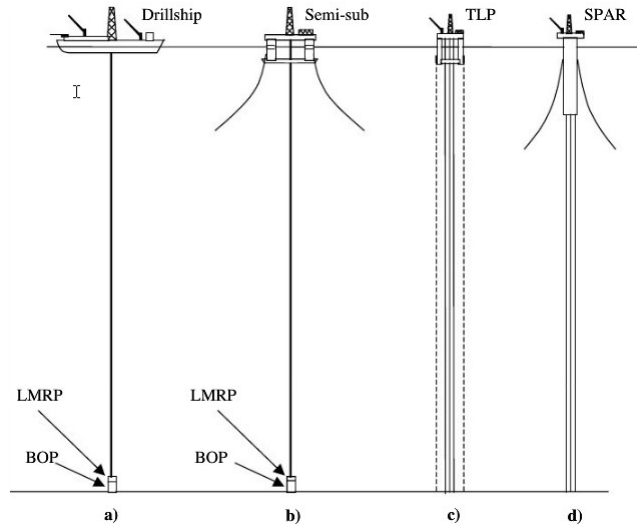
Figure 2.4: Risers deployed below MODUs, tension leg platforms, and spars[3]

in the top-tensioning riser system that keeps constant tension on the riser by expanding and contracting with the movements of the facility, as it is shown in Figure 2.5. This is a typical heave compensating system for drilling risers, and a typical stroke capacity for world wide drilling will exceed 15 meters.

The main parts of the riser tension system are hydraulic cylinders, accumulators and air pressure vessels[4]. As it is shown in Figure 2.5, normally six hydraulic cylinders are used, which are connected to the floating facility under drilling platform. At the rod end the cylinders are connected to the riser with a tension ring. The end moments on the cylinder are eliminated by using connections with shackle and eye, which allow rotation. As a result, in order the have static and dynamic equilibrium of loads on the riser, there may be different inclinations on the cylinder giving varying tension direction.

The strokes of the cylinder compensate the relative motion between the riser and the floating unit. In order to keep a certain amount of tension, the hydraulic cylinders are connected to nitrogen pressure vessels (NPV) (see Figure 2.6). The NPV acts like a soft spring with certain pre-set pressure, which give approximately constant tension to the stroke of the cylinders.

2.3 Pipe-in-pipe model of hydraulic cylinders

As it was introduced previously, the heave compensating system for drilling risers will normally be based on a set of hydraulic-pneumatic cylinders directly coupled to the riser on the tension ring. In RIFLEX program, the pipe-in-pipe model for cylinders and rods are included. The master pipe will be equipped with tubular contact components at all FE-nodes belonging to the pipe. The slave pipe will experience contact with the master pipe as discrete element loads.

The contact between two cylinders A and B is studied, the cylinder A (body) being located on the inside of cylinder B (body B), see Figure 2.7, where four different coordinate systems are defined[4]:

8
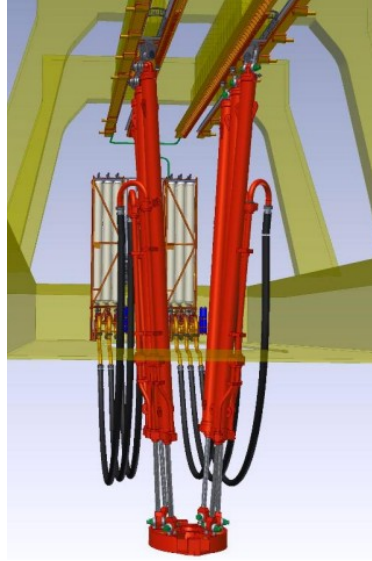
Figure 2.5: Heave compensator for drilling riser
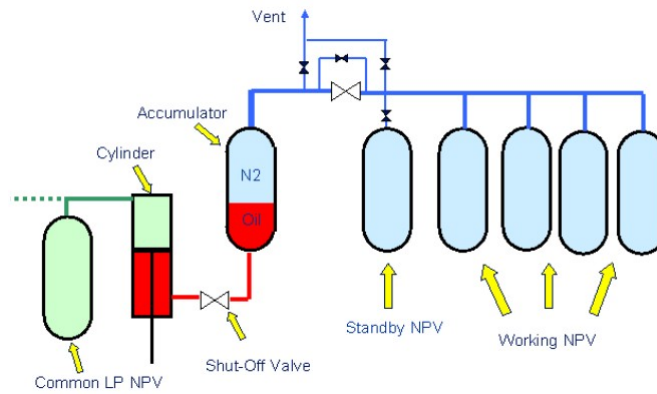
Figure 2.6: Riser tension system with NPV [4]

- The global system with axes X_i and base vectors I_i

- The master element system positioned at the centre of body A with axes x_i and base vectors i_i

- The slave element system with origo at element node B1 of slave body B with coordinate axes y_i and base vectors j_i.

- The contact point system positioned at point C on the outer circumference of the master body A with coordinate axes s_i and base vectors n_i. The outward normal n_3 is taken to be directed outward from the master body centre.

The position vector of the contact point on the surface of the master cylinder surface with radius R_A and angular orientation γ can be expressed as:

$$r_{CA} = r_A + R_A sin\gamma i_2 - R_A cos\gamma i_3$$

which in the slave body system can be expressed by:

$$r_{CB} = r_{Ba} + [R_{B1}(1-\xi) + R_{B2}(\xi)][sin\theta j_2 - cos\theta j_3]$$

Where ξ is the dimensionless length coordinate along the slave element,r_{Bi} is the radius at element end i and γ is the angular orientation expressed in the slave system. Contact is obtained when the gap g fulfils the following condition:

$$g = (r_{CB} - r_{CA}) \cdot n_3 < 0$$

It is noted that since the angle γ is not known a priori an iterative procedure is needed
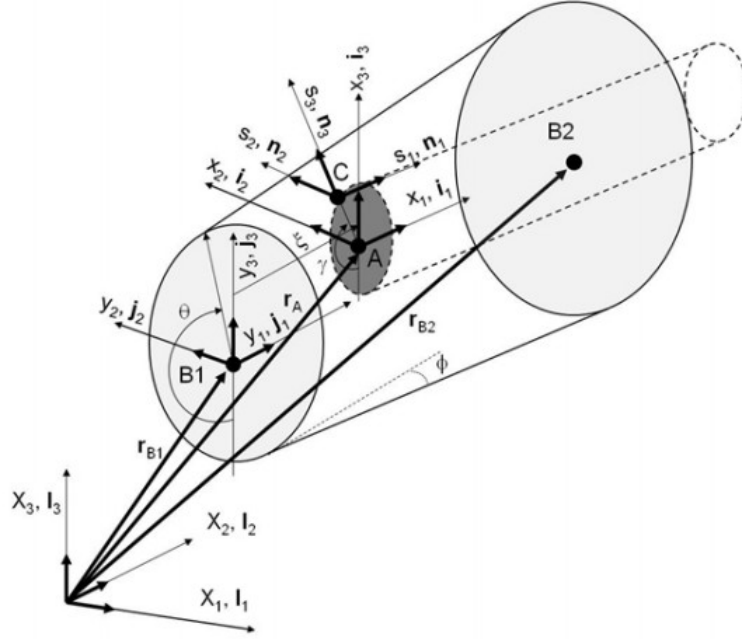
Figure 2.7: Contact element coordinate systems

to find the actual contact point.Further, if contact has been established, increments in relative slippage will occur:

$$\delta\eta_1 = (\delta r_{CB} - \delta r_{CA}) \cdot n_1 \neq 0$$

$$\delta\eta_2 = (\delta r_{CB} - \delta r_{CA}) \cdot n_2 \neq 0$$

where n_1 and n_2 are the tangent vectors defined at the contact point. The stiffness in the n_3 direction during contact is governed by application of the penalty parameter k taken to be constant or variable according to a hyper-elastic material law.

2.4 RIFLEX model

The marine drilling riser model was kindly provided by Professor Larsen, made by Ronny Sten. The drilling riser model is a complete set including BOP, heave compensation system, upper joint located beneath the drill floor and buoyancy modules modelled in *RIFLEX*. In order to accommodate the new *SIMA* version, some small modifications were needed. The layout of the model in *SIMA* was presented in 2.8. In this thesis, a more simply model without heave compensation system is enough for the extreme analysis

Table 2.1: Riser Geometry

Type	Description	Value
Marine riser	WT	22.225 mm
	OD	533.4 mm
21" OD	ID	488.95 mm
	Material	X-80(552MPa)
BOP	OD	5.5 m
	ID	476 mm
LMRP	OD	4.5 m
	ID	476 mm
Marine riser	Max OD	1371.6 mm
with buoyancy	Length	22.86 m
	Length	32.0 m
	Maximum stroke	18.3 m
Tensioner joint/	OD (outer barrel)	660.4 mm
Telescopic joint	WT (outer barrel)	25.4 mm
	OD (inner barrel)	527.3 mm
	WT (inner barrel)	19.1 mm
	OD	533.3 mm
ROPS	WT	22.225 mm
	Joint length	22.86 m

Table 2.2: Riser stack-up, 206 meters water depth

Description	Elevation [m]	Build up length [m]
Drill floor	40	
Tensioner hang-off location	37.15	
Upper flex joint	35.5	1.3
Spacer joint	34.2	12.04
Slip-joint (60' telescopic joint)	22.2	11.79
Slip-joint (75' telescopic joint)	10.4	22.86
Tensioner ring	9.9	
Mean water level	0	
ROPS	-12.5	22.86
Riser joints/pup	-35.3	20.22
Riser joints (buoyant)	-55.5	114.3
Riser joints	-169.8	22.86
Lower flex joint	-192.7	1.3
LMRP	-194	4.5
BOP	-198.5	
Bop lower end	-204	
Seabed	-206	
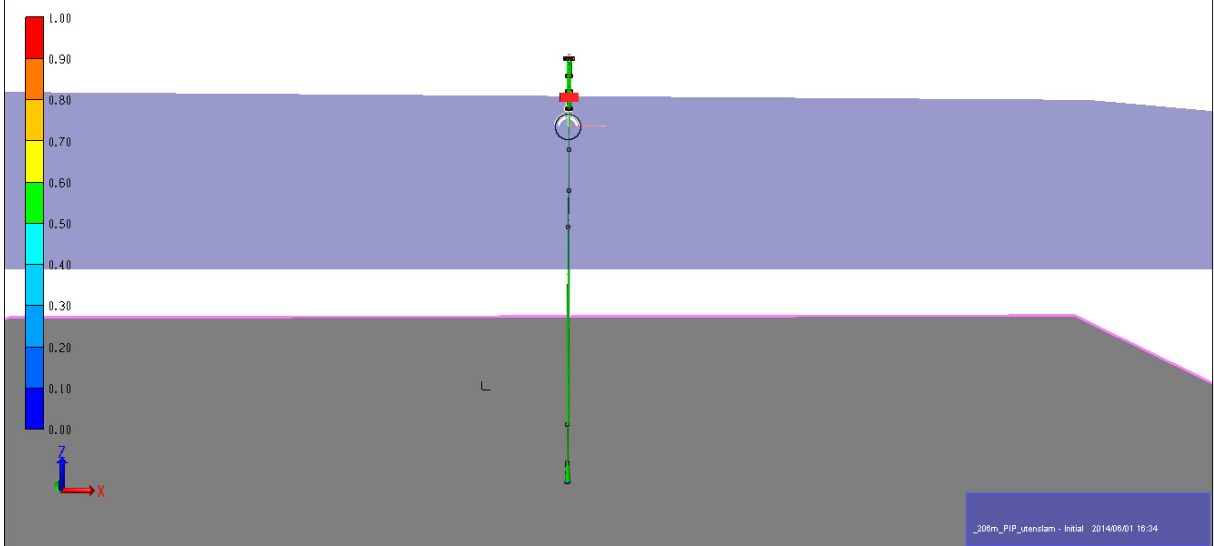
Figure 2.8: Marine Riser layout in SIMA Interface

of bending moment. For the purpose of understanding the complete drilling riser system, this model was used. The rise geometry data are presented in Table 2.1 and 2.2.

The water depth is 206 meters. The marine riser is defined from BOP to the upper flex joint. On the sea bottom the riser is connected to the well with a BOP, while the riser is linked to the heave compensation system at the tensioner ring[12]. 9.9 meters above the mean water level, the six tensioner cylinders are connected to the outer barrel of the telescopic joint, and the end of the cylinders are connected to the vessel.

2.5 Vessel motions

Since the marine riser is connected to the vessel by heave compensation system, the motions of this vessel must be known during dynamic riser analysis[13]. The motions have 6 degrees of freedom, which are surge, sway, heave, roll, pitch and yaw respectively. The vessel motion comprises a set of high-frequency motions and low-frequency motions in 6 degrees of freedom. For most dynamic analysis, only considering high-frequency motions can give enough accuracy. The high-frequency motions can be calculated by a linear approach to the wave, transfer function is used to describe the ration between wave amplitudes and vessel motions:

$$H_{HFj}(\beta, \omega) = \frac{x_j(\beta, \omega)}{\xi_a(\beta, \omega)} \tag{2.1}$$

where $H_{HFj}(\beta, \omega)$ denoted the high-frequency transfer function in a degree of freedom j, β meant wave directions while ω described wave frequency.

In this thesis, the transfer functions of six degrees of freedom were given for wave directions 0° , 22.5° , 45° , 67.5° and 90° for drilling semi-submersible *Aker Barents*. The transfer functions can be represented as discrete points in terms of wave amplitude and response amplitude, the real amplitude can be interpolated from the discrete points. They can be inserted into *SIMA* as a text file.

Chapter 3

Modelling of Irregular Wave

The ocean wave $\zeta(x, y, t)$ is a random nature both in terms of time and space. Since only the wave near the structure is of interest, the ocean wave discussed in this thesis will focus on the time series of wave at a fixed time, $\zeta(t)$, representing in a stochastic manner. In a short time period, the wave process can be assumed as a stationary process for practical reasons. However, in a long time period, this assumption could not be set up. It becomes a non-stationary process, i.e. the characteristics are no longer identical. The wave heights and spectrum peak periods are varying more than those in stationary process. Hence, in order to illustrate the characteristics of a commonly applied wave process, the long-term period wave process must be established, which is a combination of short-term wave process for practical purposes. It is convenient to establish all possible short-term distributions of wave processes, then the long-term distribution will be set up based on short-term distribution. In this chapter, both distributions and their relations will be introduced, and methods to model irregular wave will be mentioned as well.

3.1   Short-term Distribution of Waves

The probability distribution of wave heights in a wave record or within a given seastate is often denoted as short-term distribution of wave heights[5]. As it was mentioned, the sea elevation of natural wave process is idealized as a stationary, narrow-banded and Gaussian process. A stationary process means the wave characteristics are independent of time, i.e. the mean and variance A narrow-banded process means that all frequencies in the process are close to $\omega = 2\pi/T$, which means the wave period is close to the given period T_P. Thus the wave amplitude can be assumed to be Rayleigh distributed. The Rayleigh density distribution of wave heights is given by:

$$f_H(h|H_{m0}) = \frac{4}{H_{m0}^2} exp[-2(\frac{h}{H_{m0}})^2]$$
(3.1)

The ocean surface is often a combination of many regular wave components, as is shown in Figure 3.1. The wave elevation of a long-crested irregular sea can be obtained as the sum of a large number of wave components:

$$\zeta(t) = \sum_{n=1}^{N} c_n sin(\omega_n t - \varepsilon_n)$$
(3.2)

where

c_n is the amplitude of each componet, it can be either stochastic or deterministic. This will be discussed in the later section.

The phase angle ε_n is a random variable, taken from an even distribution with a internal $[0, 2\pi]$.
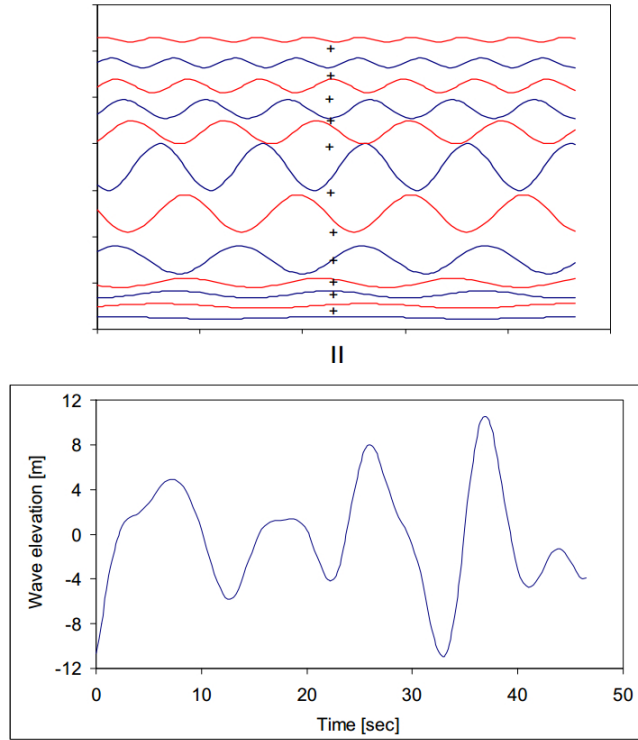
Figure 3.1: Illustration of Irregular Wave[5]

Before generating irregular wave, the amplitude of each harmony wave component has to be calculated in advance. As we assumed previously, that the sea surface is a stationary, narrow-banded and Gaussian distributed stochastic process. Such idealized wave record can be represented corresponding to wave spectrum. An example of wave spectrum was shown in Figure 3.2, which can be discrete with a constant frequency width. The deterministic amplitude generates from the spectrum density $S(\omega)$ and the corresponding frequency:

$$c_n^* = \sqrt{2S_x(\omega_n)\Delta\omega_n} \tag{3.3}$$

Wave spectrum is a complete description of surface process, which can be estimated from measurements. By applying Fast Fourier Transformation (FFT) in an observed time history, the spectrum density function can be obtained. However, large uncertainty existed because of the random nature of wave. In addition, it is too time-consuming and complicated to calculate wave spectrum for all designs, sometimes we do not have the time history to estimate the wave spectrum. Thus standard models for wave spectrum are usually applied, i.e. Pierson Moskowitz spectrum for fully developed sea and JONSWAP
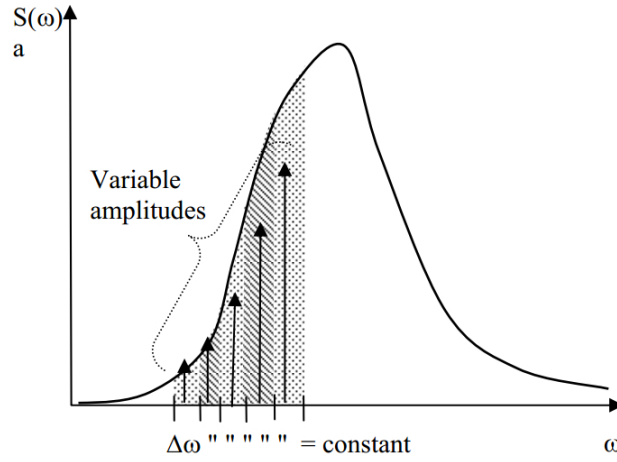
Figure 3.2: Illustration of Wave Spectrum and seastate generation[5]

spectrum for not fully developed sea. For the North Sea wave condition, JONSWAP spectrum was chosen to generate irregular waves for this case. It can be represented in terms of significant wave heigh H_S and spectral peak period T_P[14]:

$$S(f) = 0.3125H_S^2T_P^{-4}f^{-5}exp\{-1.25T_P^{-4}f^{-4}\}\{1-0.287In\gamma\}\gamma^{exp\{-\frac{1}{2}(\frac{T_Pf-1}{\sigma})^2\}} \quad (3.4)$$

The parameter σ is a measure of the width of the spectral peak, which is given by $\sigma = 0.07$ for $T_Pf < 1$ and $\sigma = 0.09$ for $T_Pf \geq 1$. F

With the obtained deterministic wave amplitudes, different methods can be used to generate wave process in a time series.

1. **Use of Stochastic Amplitude**

   If the auto spectrum of a process is known, a realization of limited duration can be represented by sine and cosine functions:

   $$\zeta(t) = \sum_{n=1}^{N}[a_n cos\omega_n t + b_n sin\omega_n t] \quad (3.5)$$

   where a_n and b_n are independent Fourier coefficient found from the Gaussian distribution with zero mean and same variance, ω_n is the wave frequency for n-th component from frequency discretization. The variance of a_n and b_n are:

   $$\sigma_{a_n}^2 = \sigma_{b_n}^2 = \sigma_n^2 = S_x(\omega_n)\Delta\omega_n \quad (3.6)$$

   This method needs N a_n and N b_n to define a sample with N frequencies. The result of this method will generate a sample of the true Gaussian distribution, but every sample has a varying variance.

2. **Use of One Stochastic Amplitude and Stochastic Phase**

This method use a cosine series with a random phase to generate samples:

$$\zeta(t) = \sum_{n=1}^{N} c_n sin(\omega_n t - \varepsilon_n) \tag{3.7}$$

This method has the same statistical property with Method 1, a stochastic amplitude c_n is:

$$c_n = \sqrt{a_n^2 + b_n^2} \tag{3.8}$$

Since a_n and b_n are Gaussian distributed with the same parameters, c_n is Rayleigh distributed with a variance equal to the sum of variance of a_n and b_n. Thus the:

$$\sigma_{c_n}^2 = \sqrt{\sigma_{a_n}^2 + \sigma_{b_n}^2} = \sqrt{2S_x(\omega_n)\Delta\omega_n} = \sqrt{2}\sigma_n \tag{3.9}$$

The Rayleigh distribution can be obtained for stochastic amplitude c_n:

$$F_{c_n}(c_n) = 1 - exp[-\frac{1}{2}(\frac{c_n}{\sigma_n})^2] \tag{3.10}$$

From the Rayleigh distribution, the stochastic amplitude can be calculated by the following procedures:

- Firstly a random number p of distribution should be picked from an even distribution with interval $[0, 1]$;

- Using the random number p to calculate the Rayleigh distribution concerning c_n:

$$c_n = \sqrt{-In(1-p)}\sqrt{2}\sigma_n \tag{3.11}$$

By introducing the relationship of σ_n to the equation, we have:

$$c_n = \sqrt{-In(1-p)}\sqrt{2S_x(\omega_n)\Delta\omega_n} = \sqrt{-In(1-p)} \cdot c_n^* \tag{3.12}$$

where c_n^* is deterministic amplitude found from the auto spectrum, it can be found from Equation 3.3.

Compared to Method 1, this method will generate the wave time records with the same statistical property. However, this method is easier to implement since it has one trigonometric function to solve and use random variables from an even distribution, while Method 1 needs to calculate two trigonometric functions.

3. **Use of Deterministic Amplitude and Stochastic Phase**

As it was mentioned in Method 2, the stochastic amplitude in the Fourier transformation will be replace by deterministic amplitude c_n^*, the transformation is shown below:

$$\zeta(t) = \sum_{n=1}^{N} c_n^* sin(\omega_n t - \varepsilon_n) \tag{3.13}$$

As is was discussed before, the c_n^* is found from auto spectrum. For infinite N, both Method 1,2 and 3 represent a Gaussian process. However, for finite N, Method 3 cannot represent a Gaussian process, while Method 1 and 2 are still Gaussian distribution. When implementing deterministic amplitude, the generated wave samples will always have the same variance as the it found from auto spectrum. Thus Method 3 does not simulate a random Gaussian process, and does not represent ocean waves correctly. It simply selects the phases of the component sine curves at random, but the amplitude is deterministic, so Method 3 will always produce a spectrum equal to the auto spectrum. Thus the randomness of the real wave system will be lost[15].

More discussion on the uncertainty of the wave generation methods will be discussed in later content.

3.2 Long-term Distribution of Waves

After constructing the short-term distribution of waves, the wave time history and wave spectrum for a given seastate can be obtained. Moreover, the variation of seastates in life time is also of interest, which is called long-term statistics. Long-term statistic illustrates the variability of the seastates which are constant in short-term statistics. As it was mentioned before, long-term distribution is a combination of short-term distribution, thus there must be a link between them. From Equation 3.1, the Rayleigh distribution of short-term distribution was presented, which can be considered a conditional distribution of h given H_{m0}. From statistics we have[5]:

$$f_{XY}(x, y) = f_{x|y}(x|y) \cdot f_y(y) \tag{3.14}$$

Thus the conditional distribution of x is:

$$f_X(x) = \int_y f_{xy} \cdot f_y(y) = \int_y f_{x|y}(x|y) \cdot f_y(y) \tag{3.15}$$

The long-term distribution of wave height h can then be given as:

$$f_H(h) = \int_{H_{m0}} f_{h|H_{m0}}(h|H_{m0}) \cdot f_{H_{m0}}(H_{m0}) dH_{H_{m0}} \tag{3.16}$$

However, this statistical derivation does not include spectrum peak period T_P. Practically, if the scatter diagram is used as a reference of seastates, the period T_P is independent of significant wave height H_S. The cumulative probability function of long-term distribution was used in this thesis, which included the influence of varying periods T_P:

$$P_X^L(x > X_D) = \sum_{i=1}^{N_S} P_X(x > X|H_S)_i \cdot P_{HT}(H_S T_P)_i \cdot g(T_Z)_i \tag{3.17}$$

where

$\quad N_S$: Number of seastates

$P_X(x > X|H_S)$: Rayleigh distribution, given H_S

$P_{HT}(H_S T_P)$: Simultaneous probability of H_S and T_P from scatter diagram

$g(T_Z)$: Weight factor introduced to account for varying T_Z from one seastate to another, introduced in Chapter 7.

T_Z : Average zero up-crossing period of sea surface

The Rayleigh distribution of wave heights is given in 3.1, which is independent of period T_P.

Normally, a scatter diagram consists of more than 100 seastates. It is expensive and time-consuming to include all seastates to response calculation with long time simulation. Long-term and short-term distribution of wave can be used as a useful tool to remove the seastate that gives insignificant influence.

The wave height which is exceeded once during m years, h_m, is of interest usually, the equation is given as:

$$1 - P_X^L(h_m) = \frac{1}{N} \tag{3.18}$$

where N is the number of individual waves during m years, given as $N = \frac{m(years)}{T_Z}$. Thus m years is called return period of h_m.

The long-term distribution of wave heights is usually represented as probability of exceedance as Equation 3.18. A sketch of probability of exceedance was given in Figure 3.3. The blue dots in the figure are the calculated results of wave heights in corresponding return periods. With enough dots, a straight line can be fitted. Hence it is convenient to find the corresponding value of wave height h for a given return period, or find the return period for a given wave height. It is noted that the fitted line of wave height and return period is not necessarily to be straight.
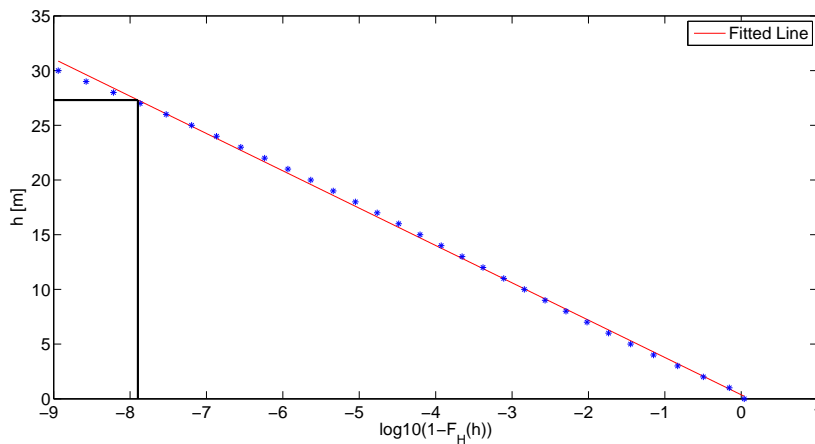
Figure 3.3: A Sketch of Long-Term Distribution

Chapter 4

Environment Loads

Tensioned risers are subjected to a variety of dynamic loads, of which the most important usually are hydrodynamic loads from waves and current and the forced motions from attached platforms or vessels[16]. Loads from fluid inside the riser, interaction with the sea floor are important for some specific discussion, but are not of interest in this thesis.

4.1 Loads From Waves

Waves can be divided into regular waves and irregular waves. Regular waves are normally modelled by two methods, both theories describe regular, long-crested waves propagating in an arbitrary direction.

- Airy linear theory

- Stock's 5th order wave theory

Airy linear wave theory was derived by assuming a horizontal sea bottom and a free-surface of infinite horizon for propagating waves. It was concluded that linear wave theory provides a good prediction of near-bottom kinematics for a wide range of relative water depth and wave steepness. The boundary condition pressure is valid at mean water level for linear theory, which means it cannot predict wave crest due to infinitesimal wave elevation assumption.

Differently from Airy linear wave theory, Stock's 5th order wave theory can consistently predict the wave induced velocity and acceleration in a wave crest. The wave profile defined by the two theories for waves of identical length and heights are shown in Figure 4.1.

The most suitable wave theory is dependent upon wave height, the wave period and the water depth. The most applicable wave theory may be determined from the Figure 4.2 which was taken form API-RP2A (American Petroleum Institute, Recommended Practice for Planning, Designing and Constructing Fixed Offshore Platforms).

Although it is easier to establish wave profile with regular wave method, it could not give a correct description of sea waves with random nature. In order to use regular wave method to simulate the sea surface, modification has to be used to modify the kinematics of the wave crest. In this way, irregular wave is a combination of harmonic components from
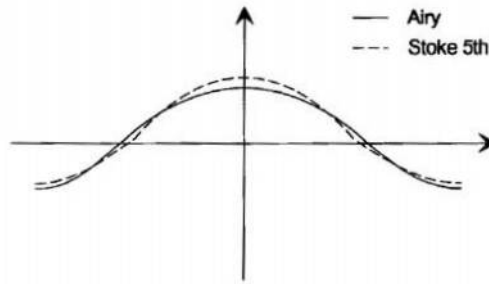
Figure 4.1: Comparison of Airy linear wave theory and Stock's 5th order wave theory
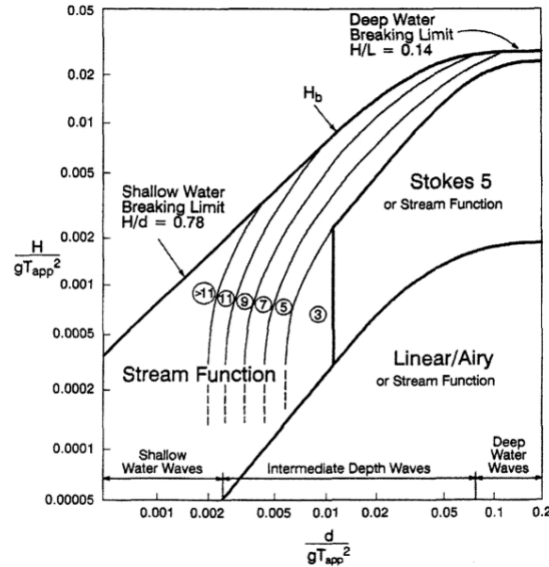
Figure 4.2: Applicability of wave theories

regular wave. The amplitudes of the components can be either deterministic or stochastic, depending on the requirements. The detailed introduction of modelling irregular waves was introduced in Chapter 3.

4.2   Loads From Current

Current is specified speed defined for different depth profiles and directions. The current velocity is normally assumed to be constant with time[6]. A quasi-static analysis can, however, include the effect from a quasi-static current variation and it is also possible to describe time dependent current variation in dynamic analysis.

The current velocity at a given position is described by the speed and direction. This can be done by giving discrete values and interpolation to actual node position or describe by current scale factor which is shown in Figure 4.3.

4.3   Modification of Airy Wave Theory

Because of the infinitesimal wave elevation assumption of Airy theory, wave kinematics can only be calculated until near mean sea level. Thus modification methods must be
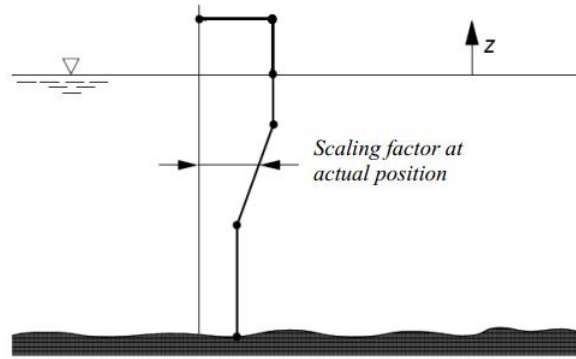
Figure 4.3: Depth profile for current speed factor coefficient[6]

introduced to calculate the wave kinematics on wave crest or trough.

In Riflex, there are four methods to modify the wave kinematics close to surface, which are[7]:

- Integration of wave forces to mean water level (method A)

- Integration of wave forces to wave surface by stretching and compression of the wave potential (method B)

- Integration of wave forces to wave surface by moving the potential to actual surface (method C)

- Integration of wave forces to wave surface by keeping the potential constant from mean water level to wave surface (method D)
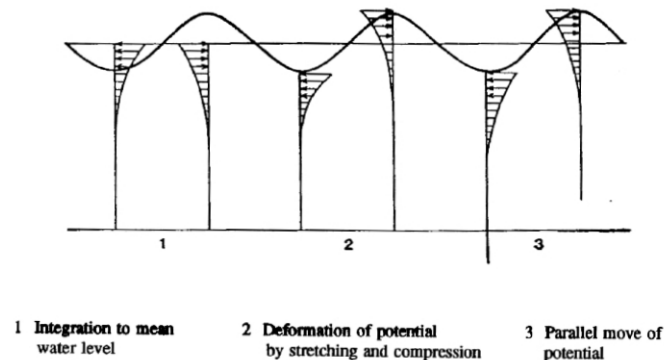
Figure 4.4: Methods to modify wave potential close to surface[7]

All the four methods are going to be introduced referring to Figure 4.4.

Method A is keeping using the assumption that the wave surface remains in mean water level. This method is included in order to have a reference point, in order to compare the results with frequency domain solutions.

Method B is always called Wheeler Stretching method, which is based on the assumption that the potential at some distance from the mean water surface is equal to the instantaneous wave surface. Hence the the potential profile is deformed by stretching and

compression according to the following foumula:

$$z' = (z - \eta)\frac{d}{d + \eta} \tag{4.1}$$

where
η is the instantaneous surface elevation.
Z' is the modified coordinate, based on Z coordinate originates at the mean surface point

Method C is a parallel move of potential, assuming that the potential is correctly described by linear wave theory, valid from the instantaneous sea surface. However, this method does not include a redefinition of potential from instantaneous sea surface to effictive water depth.

Method D means that the potential of instantaneous wave surface is always equal to the potential in mean water surface. The difference between Method A and D is that Method A assumes that the wave elevation is infinitesimal, so that the potential in mean surface can represent all wave surface. However, in Method D, the instantaneous wave surface is not necessary to be infinitesimal, the potential is equal to the mean water surface potential.

4.4 Morrison Equation

In the first two sections, hydrodynamic loads from wave and current were introduced. Normally, they are summed up as fluid kinematic in the same depth. The Morison equation is a semi-empirical equation used to calculate hydrodynamic loads on circular cylindrical structural members. It is a sum of two force components: an inertia force in phase with the local flow acceleration and a drag force proportional to the square of the instantaneous flow velocity. The Morison equation is written as[16]:

$$F_H = \frac{1}{2}\rho C_d D(u - \dot{x})|u - \dot{x}| + \frac{\pi}{4}\rho(1 + C_m)D^2\dot{u} - \frac{\pi}{4}\rho C_m D^2\ddot{x} \tag{4.2}$$

where u and $\dot{u}$ are the normal components of the fluid velocity and acceleration, x and $\dot{x}$ are the normal component of the structure velocity and acceleration. In the RIFLEX model of this thesis, the structure velocity and acceleration are set to be zero for simplicity, which means that the riser is fixed. The first term of Equation 4.2 is viscous drag force from relative velocity of fluid and structure. The last two terms are inertia forces from fluid and structure. C_d and C_m are the drag and added mass coefficient.

The hydrodynamic loads calculated by Morrison equation are nonlinear. If the drag force is dominating, frequency domain method cannot be applied in hydrodynamic loads calculation unless it is linearized. The importance of drag force depends on the ratio between the wave heights and structure diameter. If the wave heights are much larger than the structure diameter, the drag term is dominating. For riser analysis of this thesis, drag term is dominant.

Chapter 5

Dynamic Response Analysis

In the previous chapters the method of calculating hydrodynamic loads from waves and currents by applying Morison equation was introduced. However, the hydrodynamic loads are just one part of the external force in the riser, it also includes weight and buoyancy, displacements to final position of nodal points with specified boundary conditions, nodal point loads etc.. Furthermore, the external forces are not the destination to the analysis, the responses of the riser caused by the external forces are of most interest. In this chapter, methods of response calculation of tensioned riser will be discussed.

5.1   Finite Element Model

In most cases, the external forces of riser vary along time and space, i.e. the hydrodynamic loads vary along the water depth. Thus the loading from external loads may be nonlinear distributed. In addition, the properties of the riser are normally not identical in the whole structure. Hence *Finite Element Method(FEM)* is applied to divide the structure into finite element units, which give identical structure and material properties. Figure 5.1 illustrated the system division logic for applying FEM in $RIFLEX$ program[7]. $LINE$ is the biggest section, which are restrained by $SUPERNODE$ with specified boundary conditions. $SEGMENT$ is part of $LINE$ which has uniform cross section properties and element length. $ELEMENT$ is the finite element unit, it can be either bar or beam element, depending on the importance of the bending stiffness.

As it was mentioned previously, the properties of the riser are not linearly distributed. Based on the system division shown in Figure 5.1, the properties are calculated for each finite element unit. The implementation of FEM is introduced in *RIFLEX Theory Manual*, mass matrix, damping matrix, stiffness matrix and crossing section modelling etc. are given, thus the FEM model of the riser can be established. The FEM formulations should include the ability to analyse large displacement, and then large rotation as well.

5.2   Static Finite Element Analysis

After the finite element model was built, and the external loads were known, analysis of response based on FEM can be performed. Firstly static analysis was considered. The purpose of static analysis is to find the nodal displacement vector that gives a static equilibrium, which can be the starting point of dynamic analysis. The static equilibrium can

SUPERNODE   Branching points or nodes with specified boundary conditions
LINE   Suspended structure between two supernodes.
SEGMENT   (Part of) line with uniform cross section properties and element length
ELEMENT   Finite element unit
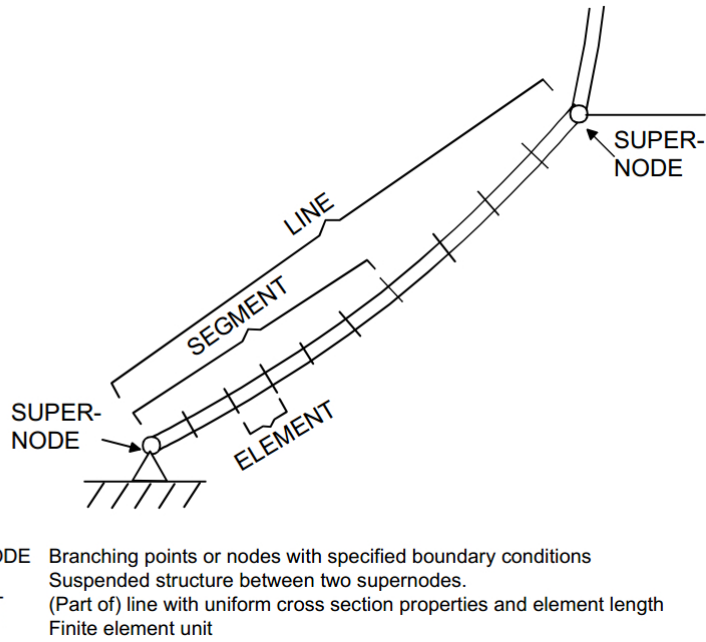
Figure 5.1: System division by FEM[7]

be given as matrix equation:

$$K \cdot r = R \tag{5.1}$$

where K is the structure's stiffness vector, r is the displacement and rotation vector, and R is the external loading vector. As mentioned previously, normally neither the loading nor the stiffness is linear distributed, thus it is not a linear equation. Numerically, Equation 5.1 is solved by application of a incremental loading procedure with equilibrium iteration at each time step.

In $RIFLEX$ program, the loading procedure of basic load types is given as[13]:

1. Volume forces (weight and buoyancy)

2. Specified displacements (i.e. displacements from stressfree configuration to final position)

3. Specified forces (nodal point loads)

4. Position dependent forces (current forces)

In $RIFLEX$ program, the sequence of applying basic load type is 1,2,3,4. After applying the volume forces, the riser is in so called stressfree configuration. For vertical tensioned risers, physical instability will occur due to the compression. It can simply be solved by adding specified tension on the upper end. The bending stiffness has limited effect in the overall static analysis, thus it is not considered.

The basic idea of static analysis is to accumulate the external loads by incremental load step. Each load step is solved by iterative solution of Equation 5.1, starting from the displacement vector of last incremental load step. There are accuracy requirement in the iterative calculation, when the error reach the requirement, the calculation will stop.

5.3 Dynamic Finite Element Analysis

In the static analysis, the system is considered to be only displacement dominated. However, in the really case, the damping and inertia forces are very factor to the analysis as well. In addition, as it was introduced previously, the external loads from hydrodynamic loads vary along time. Thus static analysis is not enough to estimate the response correctly. The general equation of dynamic finite element analysis is given as:

$$K \cdot r(t) + C \cdot \dot{r}(t) + M \cdot \ddot{r}(t) = R(t) \tag{5.2}$$

In most cases, the dynamic equation is nonliear, i.e. the Morison equation used to calculate the hydrodynamic loads is expressed by relative velocity and the vessel motions are also transferred to tensioned riser by transfer function. Hence the the structural matrices and external load vector need to be updated in each time step. The most important nonlinear effects should be considered in slender structure analysis are[13]:

- Geometric stiffness

- Nonlinear material properties

- Hydrodynamic loading calculated by generalized Morison equation

- Integration of loading to actual surface elevation

- Contact problems

In the *RIFLEX* model of this thesis, almost all the important nonlinear factors were included. For example hydrodynamic loads calculated by Morison equation based on relative velocity, modification of surface elevation using Wheeler stretching method, contact with seafloor using global spring and so on. Thus the dynamic analysis in this thesis has to be performed in a nonlinear way.

Time Domain Analysis

In previous chapter the modelling of irregular wave was discussed. It can be seen the the kinematics of the wave (maybe also current) varies along time at a fixed point in the structure. Since the Morison equation is based on relative velocity between the structure and the fluid, the external loads have to be updated in each time step. Because of the nonlinearity in the system, the stiffness, damping and mass matrices were also calculated in each time step. This is time domain analysis. The response of the structure will be obtain form each time step. If a long time domain simulation is performed, it means a large amount of response history data are also generated. Even so, since the reliability of time domain analysis is strongly influenced by simulation length, it is necessary to perform a long time domain simulation. An effective post-process method has to be applied to reproduce large amount of data according to the interest, i.e. extreme loads or fatigue estimation.

By introducing the tangential mas, damping and stiffness matrices, the incremental equation of time domain dynamic analysis was given as:

$$M_t \Delta \ddot{r}_t + C_t \Delta \dot{r}_t + K_t \Delta r_t = \Delta R_t^E \tag{5.3}$$

where M_t, C_t and K_t are the tangential mas, damping and stiffness matrices. $\Delta \ddot{r}_t$, $\Delta \dot{r}_t$ and Δr are the incremental acceleration, velocity and displacement respectively. ΔR_t^E is the incremental external force vectors. In order to solve the incremental equation, numerical integration method of dynamic equilibrium equation based on Newmark α-family was applied. A constant time step is used to divide the response in different time. Newmark α-family gives several integration methods to calculate the relationship between a time step. The general equation of the relations between displacements, velocity and acceleration vectors at time t and $t + \Delta \tau$ are given as[13]

$$\dot{r}_{t+\Delta \tau} = \dot{r}_t + (1 - \gamma)\ddot{r}_t \Delta \tau + \gamma \ddot{r}_{t+\Delta \tau} \Delta \tau \tag{5.4}$$

$$r_{t+\Delta \tau} = r_t + \dot{r}_t \Delta \tau + (\frac{1}{2} - \beta)\ddot{r}_t (\Delta)^2 + \beta \ddot{r}_{t+\Delta \tau}(\Delta \tau)^2 \tag{5.5}$$

where $\Delta \tau = \theta \Delta$, $\theta \geq 1.0$

When $\theta = 1$, it gives Newmark β-family, while Wilson θ-method is found when $\theta > 1$.

The external load is updated on each time step for time domain simulation. As it was discussed before, the hydrodynamic load is related to the velocity and acceleration of the structure. The kinematics of wave and current need to be modified in each time step to the surface elevation, to form a new velocity and acceleration profile. It makes the nonlinear time domain simulation very time-consuming. As it is finite element method, all force vectors are the contribution from the nodal force of each element. If the nonlinear hydrodynamic force is dominating the nonlinear effect of the system, the nonlinear time domain simulation can be linearized by setting the system matrices to be constant during the simulation. However, the hydrodynamic force is still nonlinear.

Frequency Domain Analysis

Frequency domain analysis requires the external forces and the displacement to be linear. This can be achieved by keeping the system matrices constant, and linearized hydrodynamic loads at the same time. Hence the dynamic equilibrium equation can be transformed into frequency domain equation[16]:

$$(K - \omega^2 M + i\omega C)r(\omega) = R(\omega) \tag{5.6}$$

Where $R(\omega)$ and $r(\omega)$ are load and response vector consist of harmonic components at each frequency.

As it was discussed previously, the load which contains hydrodynamic load is nonlinear, because of the drag term,. Thus the drag force needs to be linearized by linearization

coefficient:

$$f_D = \frac{1}{2}\rho C_d D K_L (u - \dot{x}) \tag{5.7}$$

where K_L is the linearization coefficient. To be noticed that this is the case without current. If current is included, a second linearization coefficient should be used. In addition, no modification of surface kinematics or time-varying system matrices can be included in the frequency domain simulation. Which means that for systems with nonlinear effect, frequency domain simulation will cause a more significant model uncertainty than time domain simulation.

The modelling of irregular wave is Gaussian distributed. Since the hydrodynamic load is linearized, and the frequency equilibrium equation is also linearized, both loads and responses distribution are Gaussian. For post-processing of response, there is no stochastic uncertainty in frequency domain simulation, which makes the post-processing of the response data much easier than the time domain analysis. In addition, the frequency domain calculation is much faster than time domain. A balance should be taken between nonlinear effect and convenience, to choose the better dynamic calculation method. In this thesis, the nonlinear effects were significant, thus time domain simulation were chosen.

Chapter 6

Statistics of Response

In the previous chapters, the statistical method of waves, hydrodynamic loads calculation and dynamic response analysis were discussed. After the dynamic response analysis, large amount of response data will be generated. However, response data in terms of time or frequency could not give a direct result on the interesting response, i.e. extreme response in this thesis. In this chapter, several methods used to predict characteristic loads corresponding to required annual probabilities of exceedance will be introduced. Depending on the characteristics of the response process, different statistical methods may be chosen.

6.1 Design Wave Method

For quasi-static structure with dominating stiffness, which can neglect the mass term and damping term, deterministic design wave method is a convenient tool to estimate the response. Gravity based platforms, jackets are typical quasi-static structure, they have large stiffness coefficient while low natural period. The wave condition for design wave method is q-probability wave height and corresponding wave period. The response of the quasi-static structure is determined by the instantaneous loads on the structure. In terms of maximum loads, it can be taken from the q-probability exceedance of response.

The deterministic wave height based on q-probability exceedance level can be determined from the long-term distribution of wave heights, which is shown in Figure 3.3. In many metocean design reports of various offshore fields, the q-probability wave heigh is given together with the corresponding mean wave period and 90% confidence band for wave period**??**. Once the wave height and the wave periods are decided, Airy wave theory or 5th order wave can be used to describe the regular wave process. The characteristics of Airy wave theory and 5th order Stock wave theory have been discussed before, that Airy wave theory is easy to generate but could not describe the wave kinematics on the wave crest, while the 5th is more difficult to apply but can define the wave kinematics to the instantaneous surface. To be noticed that the resulting loads of the design wave height and selected wave period should have a annual exceedance probability of q or lower. In addition, the response from q-probability wave height does not necessarily correspond to the annual exceedance probability of q.

A time domain simulation can be used to calculate the response from design wave. The load and response are calculated in each time step of simulation. The q-probability re-

sponse is obtained from the the maximum response during the simulation.

As it was mentioned that the design wave method can be applied for quasi-static structure, that is because the stiffness of these structure is so large that the dynamic effect can be neglected. For the structure with modest dynamic effects, dynamic amplification factor (DAF) can be used to compensate the dynamic effect. It is defined by the ratio of wave period and natural period of the structure.

However, even though the dynamic effect in quasi-static structure is not significant, it still exists. Thus dynamic analysis including dynamic effects will lead to a more accurate result. Nowadays the computer resources are much easier to access, it is not a barrier for dynamic analysis anymore.

6.2 Stochastic Long-Term Response Analysis

Theoretically, long-term response analysis is a more accurate method of estimating characteristic response, since it includes the changing wave conditions. However, it is not the most economical way. For a complicated nonlinear system,applying time-domain analysis to all seastates will be very time-consuming, which is not convenient in engineering's sake.

There are basically 3 different approach to estimate the characteristic long-term extreme values, which are[17]:

- all peak values

- all short-term extremes

- the long term extreme value

The first two methods are mostly used, thus the all peak values and all short-term extremes methods are going to be introduced.

All Peak Values

A peak value of a process, describing the maximum value between tow consecutive zero up-crossings. It can also be called global maxima. $F_{X_p|H_S T_P}(\xi|h_s, t_s)$ represents the conditional CDF of peak values for each short-term seastate. The equation describing long-term distribution using all peak values method can be:

$$F_{X_p}(\xi) = \int_{h_s} \int_{t_s} F_{X_p|H_S T_P}(\xi|h_s, t_s) \cdot f_{H_s T_s}(h_s, t_s) \cdot g(T_R) \tag{6.1}$$

practically, the CDF contribution of peak values can be described by Rayleigh distribution. But for strong nonlinear response, Rayleigh distribution cannot give a good fit of the peak values.

Assuming that the peak values are all independent, the peak value ξ_q with a annual probability q of being exceeded can be estimated by:

$$F_{X_p}(\xi_q) = 1 - \frac{q}{\frac{365 \cdot 24 \cdot 3600}{\tilde{T}_R}} \tag{6.2}$$

where $\tilde{T}_R$ is the average up-crossing period.

To be mentioned that the duration of seastate does not enter this equation. It focuses on every single peak value. For storm or hurricane situation, the extremes are governed by the occurrence of very few extremes. This method is going to be used in the later chapter.

All Short-Term Extremes

In this method, the conditional CDF $F_{\tilde{X}|H_S T_P}(\xi|h_s, t_s)$ of the largest peak values of each short-term condition are shown in Equation 6.3 . The number of peak values n are given under a short-term condition and a specified duration.

$$F_{\tilde{X}|H_S T_P}(\xi|h_s, t_s) = (F_{X_p|H_S T_P}(\xi|h_s, t_s))^n \tag{6.3}$$

The long-term distribution of the short-term extreme peaks is given as:

$$F_{\tilde{X}}(\xi) = \int_{h_s} \int_{t_s} F_{\tilde{X}|H_S T_P}(\xi|h_s, t_s) \cdot f_{H_S T_s}(h_s, t_s) \tag{6.4}$$

Assuming the duration of seastates is $d = \tilde{T}$, the annual probability q of being exceeded per year is given as:

$$F_{\tilde{X}}(\xi_q) = 1 - \frac{q}{\frac{365 \cdot 24}{\tilde{T}}} \tag{6.5}$$

6.3 Stochastic Short-Term Response Analysis

For a linear load-response system exposed to Guassian wave field, a full long-term response analysis can be performed without too much difficulty. The conditional distribution of global maxima can be well described by Rayleigh distribution. Thus the linear response problem can be solved in the frequency domain, by finding the response spectrum from wave spectrum and the response amplitude operator (RAO). Since frequency domain analysis takes much less time than time domain analysis, carrying out a full long-term analysis for linear system is an acceptable choice.

As it was mentioned, for a complicated nonlinear system, a full long-term analysis may need too much time in engineering perspective. Thus short-term response analysis is used to limit the number of sea states, in order to reduce the simulation time. An example which was used widely is environment contour line method. The main theory of this method is to estimate the q-probability by studying the short-term response for the most unfavourable seastate along the q-probability contour line[18]. More details about contour line method can be found in paper *Environmental Contour Lines: A Method for Estimating Long Term Extremes by a Short Term Analysis* by S. Haver and S.R. Winterstein.

Drilling tensioned riser in this case has a strong nonlinear nature, thus a full long-term analysis in frequency domain cannot be performed. In order to avoid full long-term analysis, effort has been made to reduce the number of seastates to reduce simulation time. Environmental contour line method is one example introduced, in this thesis another alternative method, simplified long-term statistic method, was applied.

Chapter 7

Simplified Long-Term Statistic Method

Simplified long-term statistic method was introduced in the early 90's by Professor Carl Martin Larsen, from Department of Marine Technology, Norwegian University of Science and Technology. This method aimed at the lifetime extreme response estimation of marine risers, by solving the nonlinearity in marine riser response. Normally long-term response statistics are only applied for quasi-static systems or linear system, in order to use long-term statistics for nonlinearity found in marine risers practically, this method combined linear frequency domain method and a stochastic time domain method.

In this chapter, the theory and procedures of this method are introduced, a tensioned riser case will be studied as well.

7.1   Introduction

During the 70's, the riser systems could be monitored, since most tensioned marine riser systems were applied from floating vessels during drilling operation. The drilling systems were operating under given environment condition, when overstress happens, the riser can be disconnected and recovered. Thus the riser elements can be easily inspected and replaced. In the 80's, a new application of the tensioned steel riser appeared in floating production units, especially tension leg platform. The first permanent riser of this kind was installed on the Hutton field in 1984, afterwards there are more and more permanent riser systems were installed. They are exposed to extreme environmental conditions as platform and it is difficult to inspect. Thus a reliable method for fatigue analysis and prediction of lifetime extreme response become necessary to deal with the new regulations given by authorities.

As it is known, the riser diameter is much smaller than the wave height, then the nonlinear drag forces will be important, described by Morison equation. Since it is nonlinear related to wave process, the response problem can not be solved in the frequency domain. The force will be experienced not only on the wave frequencies, but also on multiples of these frequencies. Similarly, since the response is non-Gaussian process, Rayleigh distribution cannot give a correct statistical result. A new strategy has to be proposed to deal with the nonlinearity of the response. The SLTS method is composed of conventional methods

such as regular wave, design storm and direct use of long-term response statistics. It is based on a combination of long-term wave statistics, use of frequency domain analyses and time domain simulations. This method is an alternative strategy for lifetime extreme response prediction, a simple flow chart of this method is presented below.

Methodology of SLTS
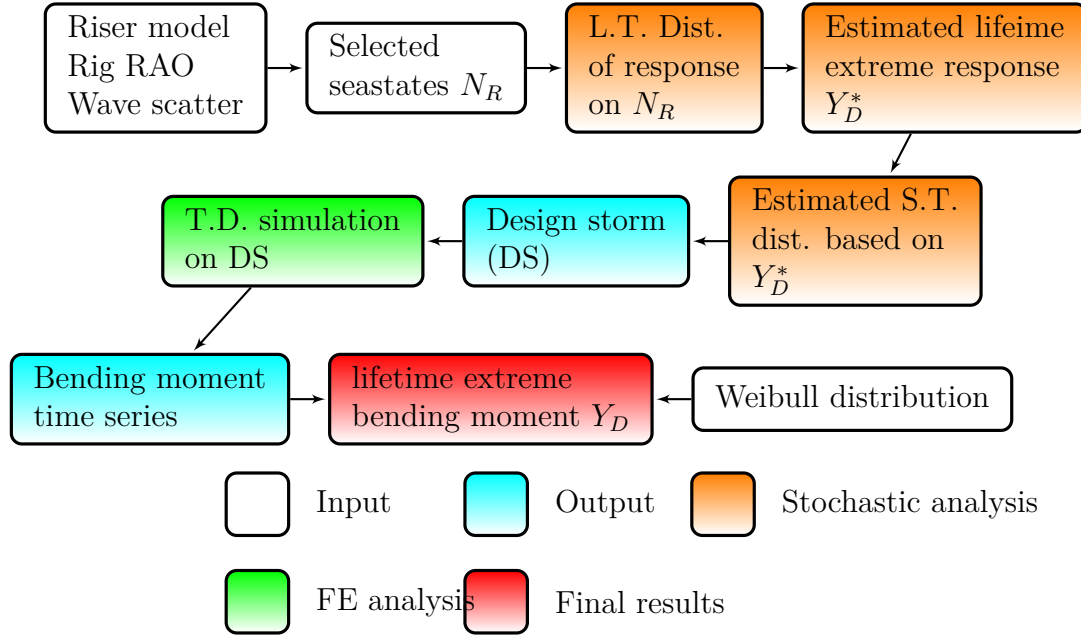
7.2 Methods for Load Effect Analysis

In this thesis, only the effects from first order wave forces are considered in the statistics of bending moment. Two alternative methods of dynamic analysis can be used to solve this kind of problem:

- Linearization of drag forces by stochastic method, then frequency domain (F.D.) method can be applied

- Direct integration in time domain (T.D.) including load iteration due to non-linear drag forces.

When applying the above methods on the present problem, the main difference is connected to statistics. The F.D. analyses can only be applied for the description of Gaussian process. In order to predict the deviation of the relative velocity correctly along the riser, the nonlinear drag forces are linearized by an iteration. However, nonlinear response process can be described in T.D. analyses, as a non-Gaussian process. In addition, the F.D. result can give a complete description of the response process since the whole frequency range is taken into account while the T.D. result only represents a sample of the response processes.

Uncertainties exist on both F.D. and T.D. methods. In terms of model uncertainty, it is larger in F.D. method than that in T.D. method. Since the nonlinear drag forces always need to be linearized in order to perform the F.D. analysis, it is impossible to

totally get rid of the model uncertainly. The statistical uncertainty only exist in the T.D. method, which can be reduced by performing long simulations. However. it makes the T.D. method much more time-consuming than F.D. method. Even though much more powerful computers are used to simulate the cases in this thesis, it is still very time-consuming. Plus a question arises constantly for this thesis is: how long simulation does it need to obtain a stable result and get an acceptable uncertainty? Especially in the T.D. analysis of the design storm. Considering F.D. analysis, how large model uncertainty can be accepted and to what extent the nonlinear load process gives non-Gaussian response? A more detail discussion will be presented later.

In Professor Larsen's previous paper, he has proved that F.D. method gives enough accuracy to the fatigue damage calculation, which means that Gaussian process is fairly correct for fatigue analyses. However, for extreme response estimation, the focus is concentrated in the tail of the distribution, which is difficult to describe by Gaussian process. Thus T.D. analyses must be performed in order to obtain reliable extreme response prediction[10].

7.3 Procedures of SLTS method

The procedures of the SLTS Statistic method are outlined in this section, which are quoted from the original paper *Extreme Response Estimation for Marine Risers* by Carl Martin Larsen and Elizabeth Passano.

1. Establish a long-term distribution of wave spectrum parameters H_S and T_P. This distribution can be expressed as simultaneous probabilities or durations (scatter diagram) based directly on observations or fitted distributions as proposed by Haver and Hyhus (1986).

2. Establish a long-term distribution for individual positive wave extremes as a weightened sum of short-term distributions. The Rayleigh distribution can be used for the short-term description if one extreme per zero upcrossing is counted. This distribution will appear as

$$P_X^L(x > X_D) = \sum_{i=1}^{N_S} P_X(x > X|H_S)_i \cdot P_{HT}(H_S T_P)_i \cdot g(T_Z)_i \qquad (7.1)$$

   This function was discussed in Chapter **??**.

3. Identify the wave amplitude X_D with return period equal to the design lifetime D (often defined as 100 years) by solving the equation

$$P_X^L(x > X_D) = 1/N_X \qquad (7.2)$$

where

N_X : Number of zero up-crossings during D years in all seastates

This equation can easily be solved by iteration.

When X_D is known, the significance of each individual seastate with regard to the found extreme value can be found by inspecting the relative magnitude of the product

$$P_X(x > X|H_S T_P)_i \cdot P_{HT}(H_S T_P)_i \cdot g(T_Z)_i \tag{7.3}$$

for all seastates. Note that the relative importance of seastates expressed in this way is dependent on the return period through the amplitude X_D. This information can be used to limit the number of seastates needed in a simplified long-term description, and hence reduce number of response analyses in the succeeding steps. Normally, 10-15 seastates should be necessary, while the complete scatter diagram contains typically 150-200 seastaes.

4. Establish an approximate long-term distribution of the response from frequency domain response analyses (including stochastic linearization). From the analyses, the response spectrum and hence the variance and average zero up-crossing period of the response is found, and the approximate distribution can again be found as a weightened sum of Rayleigh distribution:

$$P_Y^L(y > Y) = \sum_{i=1}^{N_R} P_Y(y > Y|H_S T_P)_i \cdot P_{HT}(H_S T_P)_i \cdot g(T_R)_i \tag{7.4}$$

where

N_R : Number of seastates in the approximate distribution

T_R : Average zero up-crossing period of the response

All probability distribution in Eq.7.4 are similar to Eq. 7.1

5. Calculate an approximate value of lifetime extreme response Y_D^* by solving the equation

$$P_X^L(y > Y_D^*) = 1/N_Y \tag{7.5}$$

where

N_Y : Number of response zero up-crossings during D years, counted for the N_R seastates only

Again the influence from each individual seastate can be found by computing the relative magnitude of the term

$$P_Y(y > Y_D^*|H_S T_P)_i \cdot P_{HT}(H_S T_P)_i \cdot g(T_R)_i \qquad (7.6)$$

From this information, a design storm for a given response type can be identified as the seastate with largest contribution to the long-term probability at the design response level Y_D^*. The short term probability level P_S is also found as

$$P_S = P_Y(y > Y_D^*|H_S^D T_P^D) \qquad (7.7)$$

where

$H_S^D T_P^D$: Wave spectrum parameters for the design storm

Y_D^* : Approximate lifetime extreme response

6. The final estimation of the lifetime maximum response, Y_D, can now be found from a time domain simulation in the design seastate defined by H_S^D, T_P^D. From the calculated time history a short-term probability distribution must be estimated, and Y_D be found from the equation

$$P_Y^D(y > Y_D) = P_S \qquad (7.8)$$

where

P_S : given by Equation 7.7.

P_Y^D : estimated probability distribution

The above strategy involves the following decisions and uncertainties:

- What number of seastates is needed in the simplified long-term distribution? (N_R, Eq. 7.4)

- Can F.D. results in terms of variances and average zero up-crossing periods be used to establish an approximate long-term distribution?

- How to fit a distribution to the time domain result?

- What duration is needed in a simulation in order to calculate a reliable estimate at a given probability level?

These questions will be discussed in the following sections.

7.4 Weight Function

In 7.1, the weight function was outlined, it was used to represent the weight of different seastate. If the long-term distribution was represented as:

$$\sum_{i=1}^{N} Q_i(x_a) \cdot g(H_S, T_P) = \frac{1}{N_{TOT}} \tag{7.9}$$

where $g(H_S, T_P)$ is the weight function as a function of H_S and T_P.

$$g(H_S, T_P) = P(H_S, T_P) \cdot \frac{\bar{T}_Z}{T_Z(H_S, T_P)} \tag{7.10}$$

where

$g(H_S, T_P)$: weight function;

$P(H_S, T_P)$: probability of one particular seastate with a given combination of H_S and T_P;

$\bar{T}_Z$: average zero up-crossing period;

$T_Z(H_S, T_P)$: individual zero up-crossing period.

The weight function is very important in long-term statistics in order to weight various seastates correctly. From a scatter diagram it can be seen that every seastate has different occurrences, thus different impacts due to the difference of occurrence should be accounted for. If the weight function was not or not properly included, the contribution of each seastate will be incorrect in the long-term distribution. In addition, the individual period varies in every seastate, it should be accounted for in every seastate. Thus the wave or response amplitude of N year return period will not be obtained properly without the weight function.

7.5 Long-Term Distribution of Waves

In this section, the question about choosing numbers of seastates was discussed. Scatter diagram for spectrum parameters H_S and T_P was used in all long-term wave statistics in this section. Data were taken from scatter diagram which is shown in Figure 7.3.

When we only consider extreme response, not all seastates are important. In addition, it is also time-consuming to simulate in all seastates. Thus it is important to decide the most critical seastates, instead of testing all seastates. An simulation has been perform, it shows a practical way of choosing seastates.

A marginal distribution of H_S can be found from table 7.1. The distribution is discretizing with spacing of 1 meters in the interval [0, 13m], 13 seastates were defined. The seastates are defined as H_S and numbers of occurrence during 50 years,which has equal return period as the design lifetime. By solving equation 7.2,the wave amplitude X_D can be found with return period of 50 years. The result of wave amplitude is:

$$A_{100}^M = 12.31m$$

Table 7.1: Marginal distribution of H_S

CASE NO	H_S(m)	NO. OF SEASTATES DURING 50 YEARS
1	0.50	43476
2	1.50	59302
3	2.50	25252
4	3.50	10350
5	4.50	4519
6	5.50	1882
7	6.50	753
8	7.50	292
9	8.50	110
10	9.50	40
11	10.50	14
12	11.50	5
13	12.50	2
14	13.50	1

After identifying the wave amplitude, the relative importance of each individual seastate with regard to the found extreme value can be found by equation 7.3. The result of duration and relative influence is shown in Figure 7.1. As we can see from the figure, the seastates with H_S below 9 meters contribute minor influence to the extreme probability, even though the relative duration time is dominating. Thus long-term statistics can be estimated by seastates above 9 meters only, which is shown in Table 7.2.

Considering only 12 seastates from Table 7.2 as scatter diagram, a new extreme wave amplitude with 50-year return period can be calculated by Equation 7.2. The result based on new scatter diagram is:

Table 7.2: Use of 12 seastates above 9 meters

CASE NO	H_S(m)	T_P (s)	NO. OF SEASTATES DURING 100 YEARS
1	12.50	15.50	1
2	11.50	13.50	1
3	11.50	14.50	1
4	11.50	15.50	1
5	11.50	16.50	1
6	10.50	14.50	4
7	10.50	13.50	3
8	10.50	15.50	3
9	9.50	12.50	7
10	9.50	13.50	11
11	9.50	14.50	10
12	9.50	15.50	6

$$A_{100}^{12} = 12.33m$$

The new wave amplitude calculated by 12 seastates is close to the one calculate by all seastates. Which proves that it is feasible to select crucial seastates to calculate extreme cases in long-term statistics, and it can provide sufficiently accurate result.
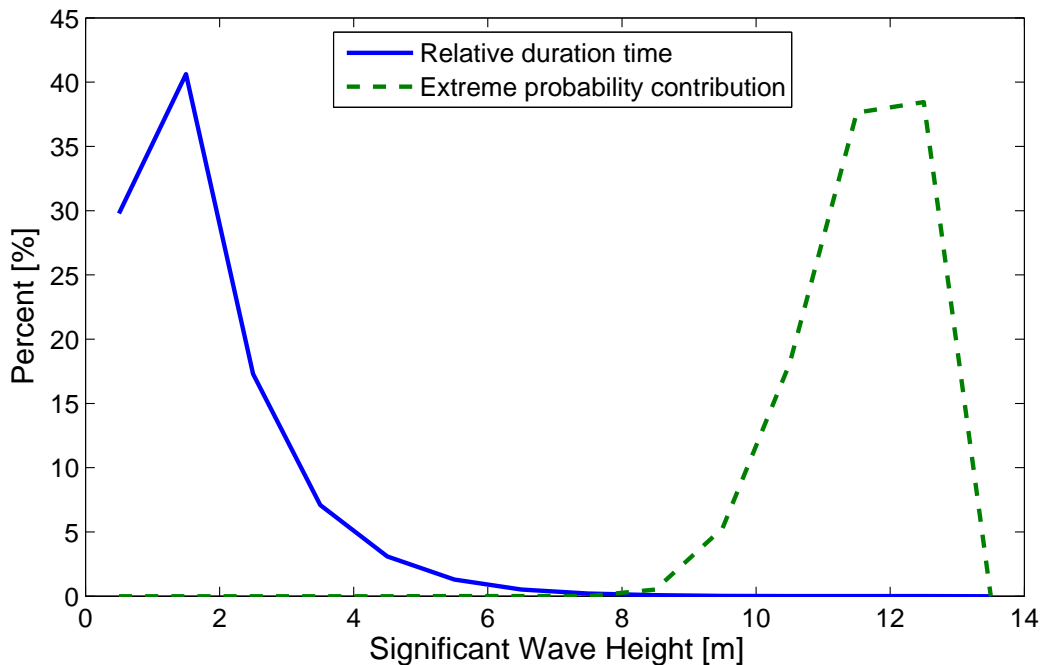
Figure 7.1: Long-Term Statistics, Influence from Seastates

Figure 7.2 shows the weight factors and the relative influence of each seastate, from these data, the dominating seastate will be identified. In addition, short-term probability is given by the application of Rayleigh distribution. Short-term probability is important

when wave statistics are used to define the design storm duration, and to decide the simulation time in time domain analyses. It can be concluded that the design storm in this case is $H_S = 12.5m$, $T_P = 15.5s$. It contributes 39.1% of the influence in long-term statistics at the wave amplitude.

Hs [m]	Explanation:							
	Case		Weigth[%]					
	Influence %		Short term prob					
9.5	9	14.29	10	22.45	11	20.41	12	12.24
	1.1	1.40E-06	1.7	1.40E-06	1.4	1.40E-06	0.8	1.40E-06
10.5	7	6.12	6	8.16	8	6.12		
	5.2	1.62E-05	6.5	1.62E-05	4.6	1.62E-05		
11.5			2	2.04	3	2.04	4	2.04	5	2.04
			10.9	1.01E-04	10.2	1.01E-04	9.5	1.01E-04	8.9	1.01E-04
12.5							1	2.04
							39.1	4.16E-04
Tp [s]	12.5		13.5		14.5		15.5		16.5

Figure 7.2: Long-Term Statistics, sea surface elevation

The method which is shown above is referred to Procedure 1 and 2 in SLTS method. The wave amplitude obtained in Procedure 2 does not represent that the extreme response will occur at this amplitude, it only means that statistically it is the most probable extreme wave amplitude. It is an important value to evaluate the contribution of each seastate, thus the most important seastates can be identified. As it was discussed previously, for extreme statistics, a certain amount of important seastates can represent the whole sea surface distribution if they are correctly selected. The most reliable way is to calculate the contribution of all seastates. However it is very time-consuming.

After discussion with my supervisor Professor Larsen, we decided to choose the seastates by his experience. Because one special condition in this case is that the riser does not have to stand the most critical seastate as the platform itself. When the seastate is harsh until a certain level, the riser would disconnect with the platform. Prof. Larsen suggested that the riser will disconnect when the significant wave height is above 7 meters. Thus the seastates with significant wave heights which are not higher than 7 meters should be chosen. The 9 selected seastates are shown in Figure 7.3. The weight, short-term probability and contribution in long-term statistics of the selected seastates are shown in Figure 7.4.

As we can see from the figure, both $H_S = 7, T_P = 11.5$ and $H_S = 7, T_P = 12.5$ contribute more than 30% to the long-term probability at a given wave amplitude. Since shorter wave period T_P is more harsh in extreme estimation, a design storm of $H_S = 7, T_P = 11.5$ should be selected. As will be discussed later, this conclusion is not in accordance with results from a simplified long-term response distribution.

H_S (m)	Spectral peak period (T_p) - (s)																			Sum
	0-3	3-4	4-5	5-6	6-7	7-8	8-9	9-10	10-11	11-12	12-13	13-14	14-15	15-16	16-17	17-18	18-19	19-20	>20	
0-1	294	1766	4314	6363	6983	6380	5180	3888	2767	1899	1271	837	545	352	227	146	94	50	110	43476
1-2	18	381	2069	5219	8233	9609	9172	7622	5745	4038	2698	1737	1089	669	405	243	145	86	125	59302
2-3	0	11	172	880	2256	3659	4343	4138	3356	2439	1621	1011	600	343	191	104	56	30	32	25252
3-4	0	0	6	77	387	1004	1643	1933	1786	1378	929	564	317	167	84	41	19	9	7	10350
4-5	0	0	0	3	38	192	501	811	920	800	557	344	184	89	40	17	7	3	2	4519
5-6	0	0	0	0	2	20	97	249	387	411	325	205	107	49	20	7	2	1	0	1882
6-7	0	0	0	0	0	1	10	50	122	177	159	118	63	28	10	3	1	0	0	753
7-8	0	0	0	0	0	0	1	6	26	59	75	63	37	16	6	2	0	0	0	292
8-9	0	0	0	0	0	0	0	0	4	14	27	30	21	10	4	1	0	0	0	110
9-10	0	0	0	0	0	0	0	0	0	2	7	11	10	6	2	1	0	0	0	40
10-11	0	0	0	0	0	0	0	0	0	0	1	3	4	3	1	0	0	0	0	14
11-12	0	0	0	0	0	0	0	0	0	0	0	1	1	1	1	0	0	0	0	5
12-13	0	0	0	0	0	0	0	0	0	0	0	0	0	1	0	0	0	0	0	2
13-14	0	0	0	0	0	0	0	0	0	0	0	0	0	0	0	0	0	0	0	1
14-15	0	0	0	0	0	0	0	0	0	0	0	0	0	0	0	0	0	0	0	0
Sum	312	2158	6561	12542	17898	20866	20948	18697	15124	11217	7692	4923	2978	1735	992	566	325	189	276	145097

Figure 7.3: Scatter diagram for a period of 50 years, duration of seastate is 3 hours

7.6 Time Domain VS. Frequency Domain Results

In Section 1.4, a question was raised: Can frequency domain results in terms of variances and average zero up-crossing periods be used to establish an approximate long-term distribution? Carl Martin Larsen and Elizabeth Passano have performed model tests on a 20 inch tensioned steel riser, in order to compare the results from time domain analyses and frequency domain analyses. Four response parameters are used in this study. They are horizontal displacements and bending moments at 5 and 110 m waterdepth.

All 13 seastates have been analysed in the frequency domain. And for 6 of these, time domain simulations have been carried out. The time domain analyses consist of 8192 steps of 0.25 s giving simulations of 34 minutes, except two of them was extended to 136 minutes.

Results from F.D. and T.D. analyses show that the F.D. analyses agree well with the T.D. results. The difference in standard deviation varied between $\pm 12.4\%$ and $+9.5\%$ (in percent of the time domain values) and was mainly within $\pm 5\%$. Good agreement is also found for the mean response and zero up-crossing period. (Carl Martin Larsen, 1990).

In this thesis, time domain and frequency domain results comparison cannot be performed, since there is no frequency solver in *SIMA* Program. The only way to find the variance and zero up-crossing period in response spectrum is to use time domain solver for all selected seastates. In order to establish an approximate long-term distribution of the response, time domain simulations for all selected seastates were performed to find the variance and zero up-crossing period. The problem is put forward: how long is the duration of the time domain simulation, in order to find reliable variance and zero up-crossing period?

This problem was solved by performing a very long time simulation, to find a stable point for the variance along time. As we can see from Figure 7.5, the variance become stable after 2400 seconds (40 minutes). In addition, although the response amplitude on each seastate is different, they have similar trends in terms of variance. It is because the same seed value is applied for all simulations, the generated waves for the riser has similar trends, which give similar variance along time. A sensitivity study on how seed values influence the result will be discussed later. Thus we can perform a long simulation on only one seastate to find the stable variance. The variances are found for all 9 seastates, which is shown in Figure 7.6.
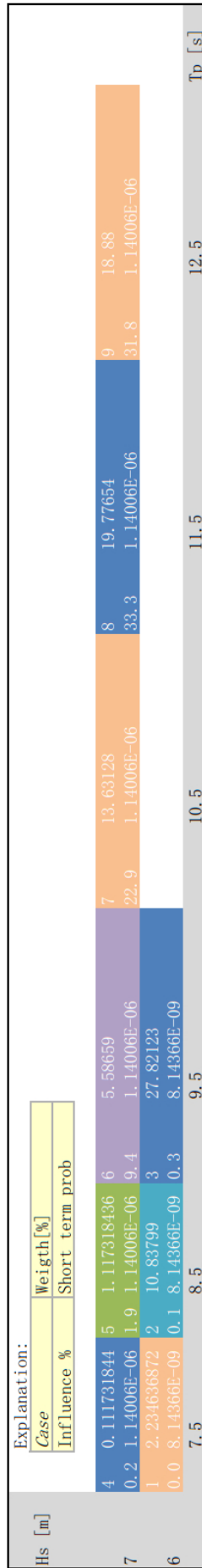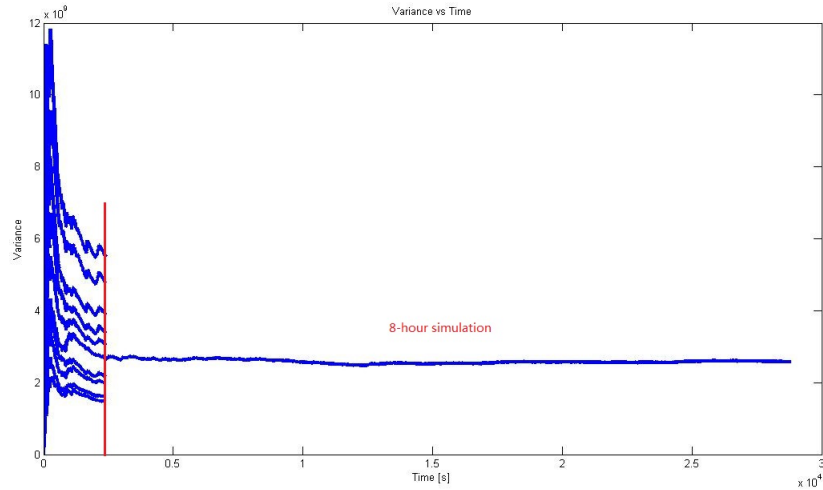
Figure 7.4: Long-Term Statistics, sea surface elevation of thesis case

Figure 7.5: Variance VS. Time for 8-hour Simulation
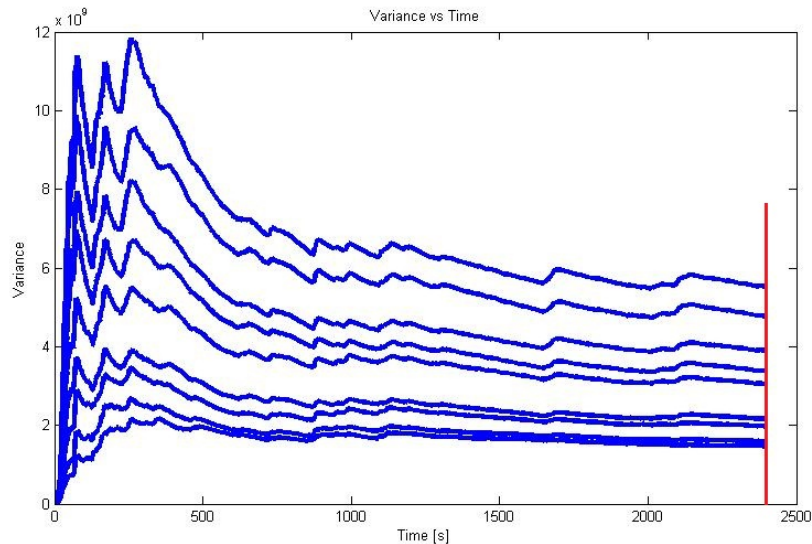
Figure 7.6: Variance VS. Time for 9 seastates, duration 40 minutes

7.7 Long-Term Distribution of Response

From the time domain analyses in the selected 9 seastates, approximate long-term distributions for the response parameters of concern were established. Each short-term distribution is of Rayleigh type, which was defined by the variance calculate from the time domain simulation. Zero up-crossing periods were calculated as well.

From long-term distribution, the response amplitude can be calculated for a 50 years return period. Then the most significant seastate can be identified for bending moment. It should be mentioned that for different response type, the contribution of each seastate may be different. In this thesis, maximum bending moment is the only response type to be of concern, thus the different response contribution of different response types can not be compared. Professor Larsen has performed a simulation on steel riser at 5 meters and 110 meters waterdepth, results on displacement and response have shown different

dominating seastates [10].

Figure 7.8 shows the result of long-term statistics of maximum bending moment. It can be seen that seastate 5 is the dominating one on the total probability, which contributes 52% of the total influence. However, the short-term probability of seastate 4 is five times higher than that in seastate 5. The reason of lower contribution in the total probability is low weight factor. When considering extreme response, short-term probability is more important, since it gives the probability of exceedance. Thus seastate 4 should be selected as design storm of maximum bending moment. Comparing long-term statistics on sea surface elevation (Figure 7.4) with long-term statistics on maximum bending moment (Figure 7.8), we can see that the most significant seastates in wave statistics is not in accordance with the results from a simplified long-term response contribution. In other words, the most harsh sea surface elevation may not cause the most critical response.

To be mentioned that the maximum bending moment in different location of the riser during the simulation is shown in Figure 7.7. As we can see that the maximum bending moment of the whole riser occurred near sea surface (excluding the connection between riser and wellhead). A.D. Trim[19] discussed that the greatest stresses depend weakly on the water depth but strongly on fluid loading near the riser top, which means that the wave elevation is a more important factor in terms of largest moment magnitude.
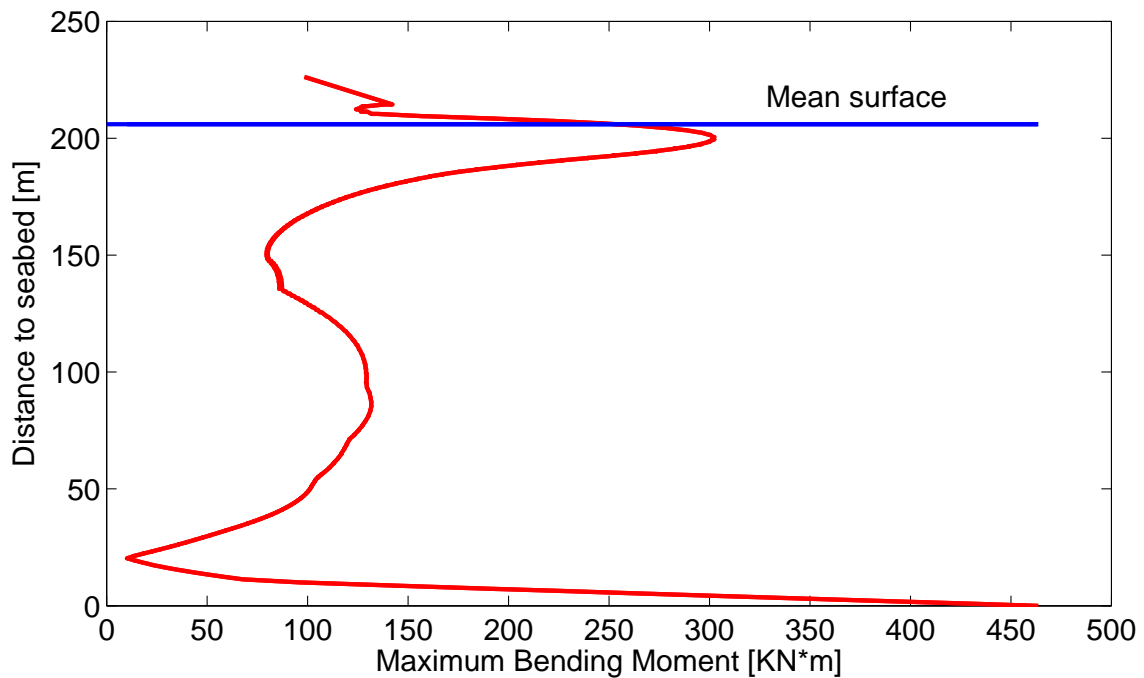
Figure 7.7: Moment envelope example of dynamic analysis

7.8 Skewness and Kurtosis

In the short-term time-domain calculation of each seastate, the skewness γ_1 and the kurtosis of response can be obtained. Skewness is a measure of the asymmetry of the probability distribution. If it is negative skew, the left tail of the probability distribution is longer,

Explanation:

Case	Weigth [%]
Influence %	Short term prob

Hs [m]		7.5	8.5	9.5	10.5	11.5	12.5	Tp [s]
7	Case	4	5	6	7	8	9	
	Influence %	27.52	52.36	0.65	0.00	0.00	0.00	
	Weigth [%]	0.001553859	0.01236164	0.05456	0.12156	0.16119	0.13839	
	Short term prob	0.00119955	2.86679E-05	8.03236E-08	1.14639E-11	2.84413E-14	2.22291E-15	
6	Case	1	2	3				
	Influence %	12.71	6.76	0.00				
	Weigth [%]	0.030966689	0.11997	0.27383				
	Short term prob	2.77954E-06	3.81482E-07	9.50463E-11				

Figure 7.8: Long-Term Statistics, Maximum Bending Moment

the mass of the distribution is concentrated on the right, or vice versa for positive skew.

The kurtosis γ_2 is defined as the fourth central moment of the response distribution normalized by standard deviation of the process. It tells the shape of the tail of the probability distribution, which can be used as a measure of the linearity of the response. For zero skewness, the process will have larger extremes than those predicted by the Gaussian distribution if $\gamma_{>}3$, which also means that the tail is higher than for a Gaussian distributed variable; and lower extremes than the Gaussian distribution for $\gamma_{<}3$.

Table 7.3: Skewness and Kurtosis of All Selected Seastates

$H_S[m]$	$T_P[s]$	Skewness	Kurtosis
6	7.5	0.3154	3.8766
6	8.5	0.3078	3.7952
6	9.5	0.2080	3.3955
7	7.5	0.3995	4.0050
7	8.5	0.3806	3.9172
7	9.5	0.2783	3.5087
7	10.5	0.3814	3.8199
7	11.5	0.3428	3.6962
7	12.5	0.1478	3.2552

Table 7.3 shows that skewness and kurtosis of response process for all selected seastates, we can see that the kurtosis are all higher than 3. It means that the response process of maximum bending moment is non-Gaussian distribution anymore, thus the distribution of maximas cannot be represented correctly by Rayleigh distribution.

7.9   Filtering of Data

After completing the steps above, design storm of the response can be obtained. Every response type may have different design storms, here the design storm was only chosen for bending moment. In order to collect more accurate result, an 8-hour simulation was performed for the design storm, even though the duration of the seastate is only 3 hours.

In order to exclude the transient effect in the beginning of the simulation, 200 seconds are added to 8-hour simulation length, for eliminating the response from the first 200 seconds. Each time step is 0.25 second, thus 116000 time steps are generated. In this thesis, only extreme values are of interest, the maxima from the response time history will be selected.

A Matlab code was generated to filter the original time history data. Firstly, simulation time of all zero up-crossing point was found. Then the largest value in each zero up-crossing interval can be determined, which is the global maxima. If there is only one maxima and one minimum between each up-crossing period, the time series is caled *narrow-banded* process. In this case, we can see from Figure 7.9, more than one maximum or minimum are existed. This is called *broad-banded* process. In broad-banded process, only the largest value in the maxima are of interest in extreme estimation, which is called global maxima. In this way, all the global maxima between each zero up-crossing point

can be obtained. Figure 7.9 illustrated the global maxima in the original time history data.
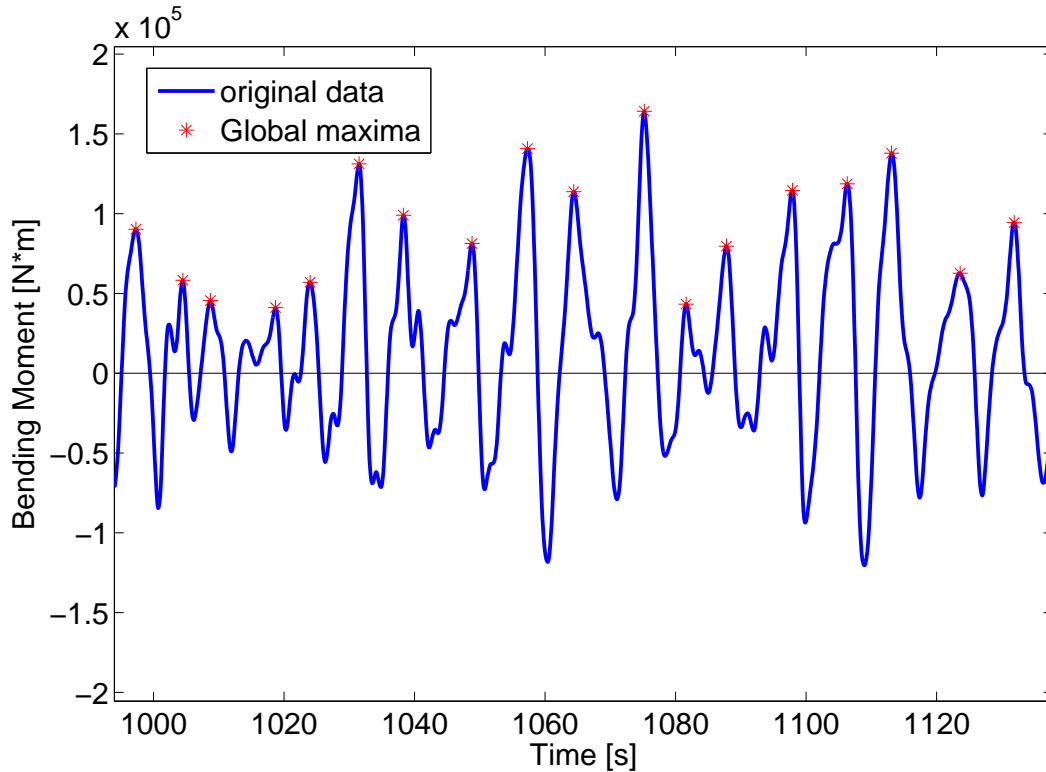
Figure 7.9: Filtered global maxima in the time history data
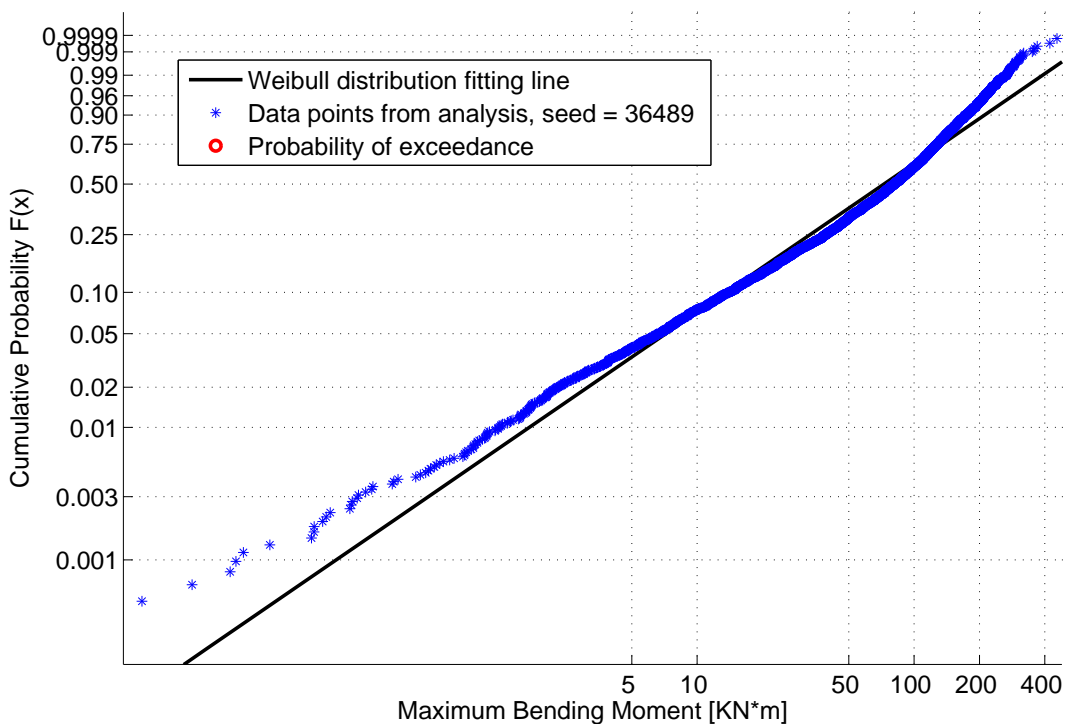
7.10   Distribution Fitting

From the simulated time series of response, the statistical properties such as mean value, variance, skewness λ_1 and kurtosis λ_2 can be calculated. Among them skewness and kurtosis are very important for selecting the distribution for the process and individual maxima. If $\lambda_1 = 0$ and $\lambda_2 = 3$, the process is Gaussian process. Then the individual maxima distribution can be described by Rayleigh distribution even the distribution is broadbanded[10].

A 8-hour simulation of the design storm $H_S = 7, T_P = 7.5$ was performed, which gave 115200 data points (seed=36489), excluding the first 200 seconds transient period. After filtering of maxima described in last section, 6153 maxima points were selected.

Two-Parameter Weibull Distribution

Figure 7.10 illustrated the distribution fitting using two-parameter Weibull distribution technique. As we can see the original data corresponded to a convex, both the lower tail and upper tail could not be described correctly. This may be caused by the shortcoming of two-parameter Weibull distribution, which is that the λ_1 and λ_2 parameters are coupled through their dependence of the shape parameter. The tail of the extremes from a nonlinear system will be strongly influenced by the nonlinear effects. However the main

part of the amplitude will be slightly influenced. Thus, if the total data was fitted as Figure 7.10, the distribution will be dominated by the linear part. The tails may not have a good fit. In order to overcome the incorrect fitting on the extreme and nonlinear part, *Tail Function* method was proposed. This method only takes the largest extreme points as a distribution for extreme estimation. The linear part which dominated the distribution will be eliminated and only the tail will be fitted. However, tail function method cannot be applied with few extremes in a sample. From experience that if 10% largest extremes are used for fitting, at least 4000 extremes are needed in a sample[10]. It is assumed that the number of extremes is enough since more than 6000 extremes were obtained from filtering.

Figure 7.10: Distribution fitting using **two-parameter** Weibull distribution fitting for all maxima points

Three-Parameter Weibull Distribution Fitting

In order to avoid concave or contex in the distribution fitting, location parameter was introduced to Weibull distribution, the distribution becomes three-parameter Weibull distribution. The extreme points will move horizontal to lower value. Since logarithmic scale is used for linearizing variables, lower sample values are easier to form a straight line on Weibull distribution paper. The cumulative distribution function for the three-parameter Weibull distribution was presented:

$$y = x - \mu \tag{7.11}$$

49

$$F(X) = P(x) = 1 - exp\{-[\frac{(x-\mu)}{\lambda}]^\gamma\} \tag{7.12}$$

where

x - statistical variable

μ - location parameter

λ - scale parameter

γ - shape parameter

Estimation of the parameters in a three-parameter Weibull distribution model will generally be rather laborious. If the location parameter θ is known, the sample { $x_1,x_2,......,x_n$ } can be transformed to { $y_1,y_2,......,y_n$ } by Equation 7.11. Then a two-parameter Weibull distribution can be applied to the sample, a rough estimation of the parameters can be found from a Weibull probability paper by plotting the transformed sample { $y_1,y_2,......,y_n$ }. If the location parameter μ is unknown, different values can be tried and the one that is closest to the straight line can be selected. However, it is difficult to apply it to many analyses by pure manual testing. In this thesis, the location parameter is found by statistical software *ReliaSoft*[20]

Alternatively, numerical method can be used to find the three parameters by moment estimators. The three first moments given by mean, variance and third order moment respectively are given below[21]:

$$E[x] = \mu + \lambda\Gamma(1 + \frac{1}{\gamma}) \approx \frac{1}{N}\sum_{i=1}^{N}x_i = \hat{E}[x] \tag{7.13}$$

$$Var[x] = \lambda^2[\Gamma(1 + \frac{2}{\gamma}) - \Gamma^2(1 + \frac{1}{\gamma})] \approx \frac{1}{N}\sum_{i=1}^{N}(x_i - \hat{E}[x])^2 = \hat{Var}[x] \tag{7.14}$$

$$m_3 = \lambda^3[\Gamma(1 + \frac{3}{\gamma}) - 3\Gamma(1 + \frac{1}{\gamma})\Gamma(1 + \frac{2}{\gamma}) + 2\Gamma^3(1 + \frac{1}{\gamma})] \approx \frac{1}{N}\sum_{i=1}^{N}(x_i - \hat{E}[x])^3 = \hat{m_3} \tag{7.15}$$

where $\Gamma(x)$ is the Gamma function of x, which is defined by:

$$\Gamma(x) = \int_0^\infty t^{x-1}e^{-t}dt \tag{7.16}$$

From Equation 7.14 and 7.15, a new function can be found with respect only to shape parameter γ:

$$\hat{Var}[x]^{\frac{3}{2}}[\Gamma(1+\frac{3}{\gamma})-3\Gamma(1+\frac{1}{\gamma})\Gamma(1+\frac{2}{\gamma})+2\Gamma^3(1+\frac{1}{\gamma})]-\hat{m_3}[\Gamma(1+\frac{2}{\gamma})-\Gamma^2(1+\frac{1}{\gamma})]^{\frac{3}{2}}=0 \quad (7.17)$$

By solving Equation 7.17, the shape parameter γ can be obtained. Inserting γ to Equation 7.13 and 7.14, the other two parameters can be found by the following equations:

$$\lambda = \{\hat{Var}[x][\Gamma(1+\frac{2}{\gamma})-\Gamma^2(1+\frac{1}{\gamma})]\}^{-\frac{1}{2}} \quad (7.18)$$

$$\mu = \hat{E}[x] - \lambda\Gamma(1+\frac{1}{\gamma}) \quad (7.19)$$

With these equations, all the parameters can be found. In order to check the fitting visibly, the original data was plotted to Weibull probability paper, thus the data needs to be transformed by linearized equations from Weibull distribution. The linearized variables are:

$$\widetilde{X} = In(x-\mu) \quad (7.20)$$

$$\widetilde{Y} = In[-In(1-P)] \quad (7.21)$$

Then the original Weibull distribution curve is transformed into a straight line:

$$\widetilde{Y} = \gamma[\widetilde{X} - In(\lambda)] \quad (7.22)$$

Examples of two-parameter and three parameter Weibull probability plot were presented in Figure 7.11 and Figure 7.12 for 45% limit for seed 36489. Here by 45% limit it means that only the data points which are larger than 45% of the largest point are selected. In this case, 306 data points are selected to plot in the Weibull distribution paper from the filtered 6153 maxima points.

As it is shown in Figure 7.11, the original data could not fit the Weibull linearized line properly, the data points formed a concave (or contex) in the distribution fitting. As it was mentioned before, this problem can be improved by adding a location parameter to the distribution, which becomes a three-parameter Weibull distribution. The location parameter was calculated by Equation 7.19, which was 204061 in this case. Figure 7.12 showed that the three-parameter Weibull distribution can give a much better fitting, the data points basically followed the straight line.
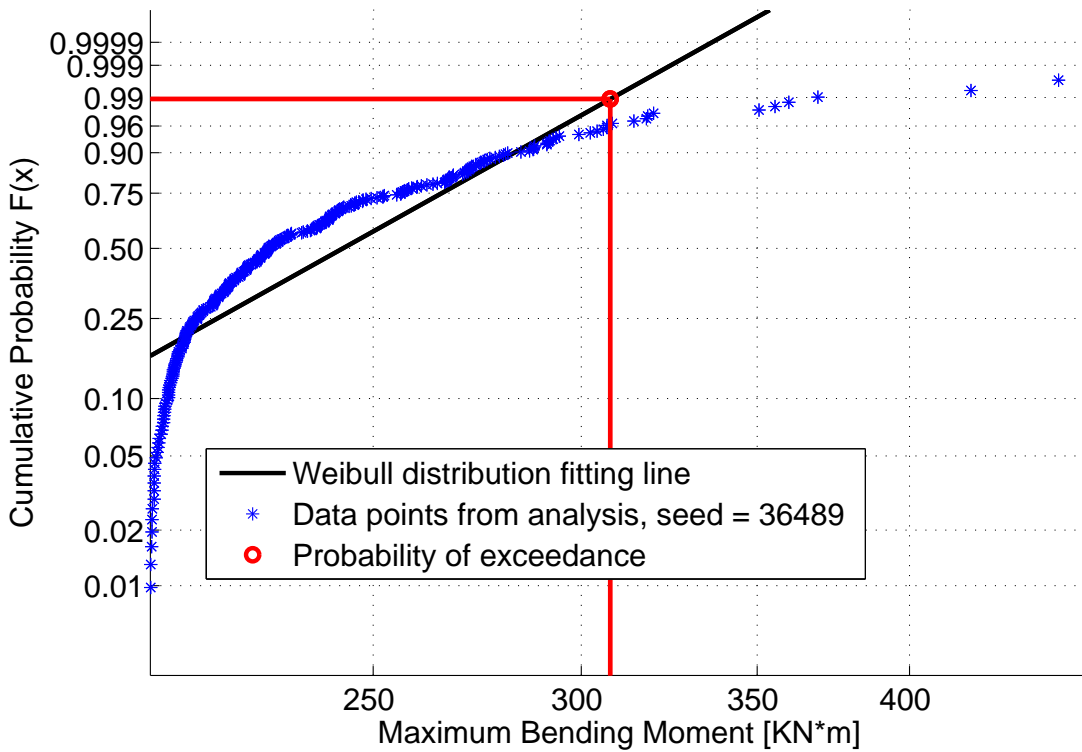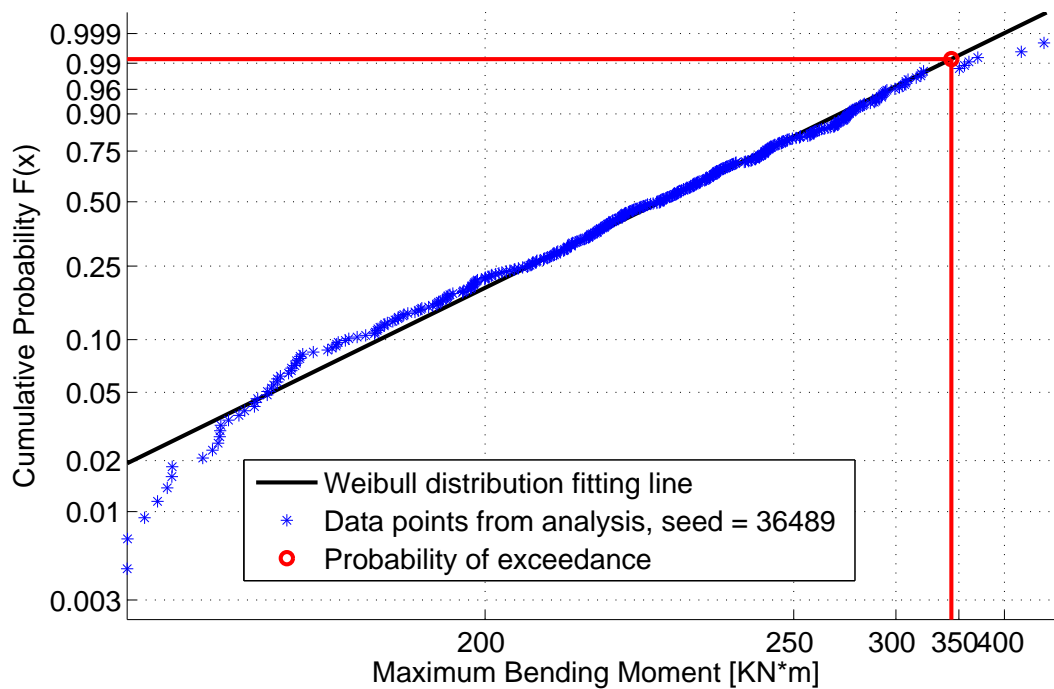
Figure 7.11: Distribution fitting using **two-parameter** Weibull distribution fitting for 45% limit
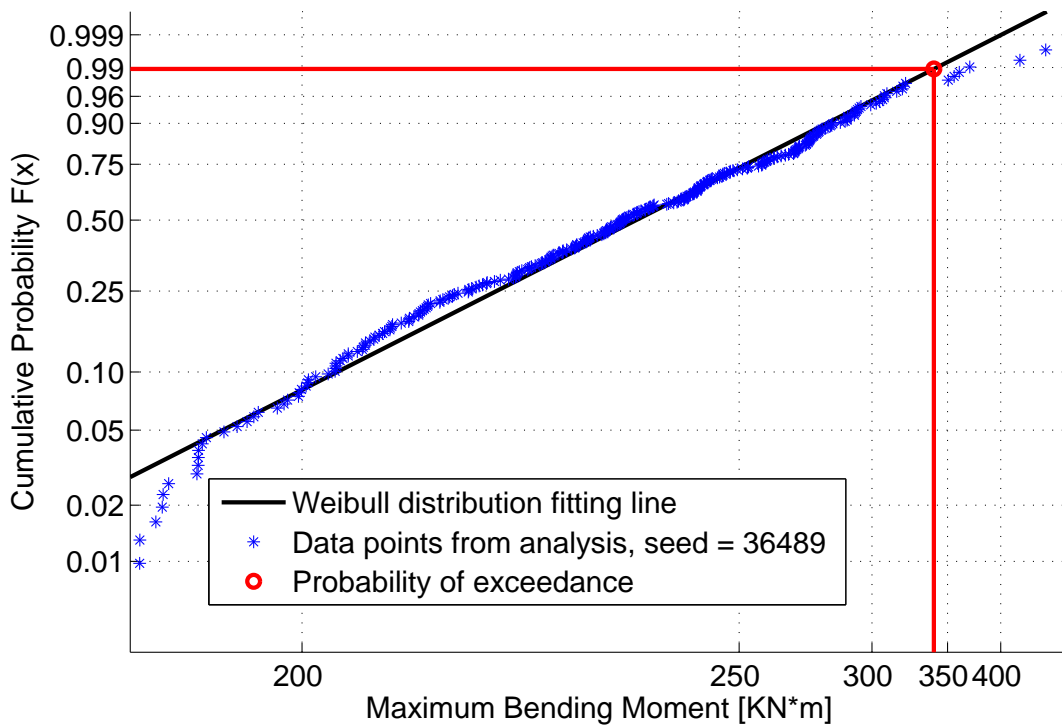
Figure 7.12: Distribution fitting using **three-parameter** Weibull distribution fitting for **45%** limit

To be noticed that the probability of exceedance should be scaled in tail function approach, since the number of data points was reduced.

From the final step of the SLTS method procedures, we know that the final estimation of the lifetime maximum response in return period of 50 years can be found from the short-term probability distribution of the designed storm, by setting the probability of exceedance equal to the short-term probability of the design storm. Since the three parameters of the distribution were calculated, the lifetime extreme response can be obtained by the function of three-parameter Weibull distribution. It can be seen in Figure 7.12, the horizontal and vertical red line are probability level and lifetime extreme response respectively.

Figure 7.13: Distribution fitting using **three-parameter** Weibull distribution fitting for **42**% limit

Sensibility Study on Limit Percentage

In order to identify how many percent limit should be chosen by tail function method, an sensitivity study was performed. A 42% limit extremes with the same seed number was chosen to fit the three-parameter Weibull distribution, which is represented in Figure 7.13. Visually, it is difficult to distinguish which one is a better fitting. Hence the mean of sum of squares due to error (SSE) was introduced to define a better fitting:

$$SSE = \frac{\sum_{i=1}^{N}(y_i - \widetilde{y}_i)^2}{N} \tag{7.23}$$

SSE means the level of error in the fitting, a smaller SSE value means a a better fitting. Table 7.4 showed the comparison of SSE value, number of data points and lifetime maximum bending moment (x50) between 42% and 45% limit, in order to find a better distribution fitting. The result showed that the 42% limit had a smaller SSE, thus the result from it should be chosen.

Table 7.4: Comparison of SSE value and result for 42% and 45% limit of the largest response, with seed=36489

Above max% included	NO. of data points	SSE	x50 [KN·m]
42	434	0.0288	491.90
45	306	0.0398	487.04

7.11   Simulation Uncertainties

There are two main reasons may lead to simulation uncertainties, which are model uncertainty and statistical uncertainty. It is very important to understand the root of the uncertainty, in order to reduce it. In SLTS method, the main uncertainties are listed below.

Transient Period

In time domain analysis, there will be a transient phase in the simulation. Thus the beginning period of the simulation should not be included until damping has eliminated the influence from the initial condition. In all the simulations for this thesis, the results from the first 200 seconds' simulation are not considered.

Irregular Generation Method

In the beginning of the numerical simulation, wave records must be generated in irregular waves. The method of simulation consisted of summing a finite number of Fourier components to obtain the surface elevation as a function of time. The three methods of generating waves are introduced in Chapter *Modelling of Irregular Wave.*

Since the wave sample generated by deterministic amplitude and stochastic phase angel will not be Gaussian distribution, the statistic distribution of extremes will not be correct. Compared to the true Gaussian wave samples, it will have difference in the individual maxima. This is an important shortcoming when second order wave force and the variability of the extreme response are considered. However, this thesis only deal with first order response and deterministic amplitude method can give a correct distribution of individual extremes, the statistical uncertainty compared to stochastic amplitude can be accepted. In addition, deterministic amplitude method is more simple and less time-consuming, thus it was used to generate waves in this thesis.

Phase Angle of Wave Generation (Seed Value)

When using deterministic amplitude method, the phase angles ε_n are independent stochastic variables taken from an even distribution in the interval $[0, 2\pi]$, a seed value needs to be used in a random number generator to generate phase angles. Thus, different seed value gives different wave samples, which leads to an uncertainty in the response. 9 seeds are used to generate wave time series for 8-hour simulations with design storm $H_s = 7m$ and $T_p = 7.5s$. The statistic property of all simulations of different seeds are presented on Table 7.5 . As we can see, the variances from the simulation of all seeds are close. Theoretically, for deterministic amplitude and stochastic phase angle method, the variance of the generated wave samples should be identical. Since this is the variance of response, it may happen that there are statistical errors or nonlinear effects would influence the final response results. But since the variances are very close, we can include that it follows the trend of identical variance. From the diversity of skewness and kurtosis values, we can know that the shape of the response distribution is different. Especially from the kurtosis we know the the tail of the distribution is different. This is very important from extreme response analysis, since the tail decides what is the extreme condition for the response. Furthermore, in order to check how much difference in the tail of the response distribution,

Table 7.5: Comparison of Variance, Skewness and Kurtosis for all seed values

Seeds	Variance	Skewness	Kurtosis
1	6.3430e+09	0.1887	3.2583
3	6.4629e+09	0.1827	3.3089
7	6.3010e+09	0.1614	3.2246
13	6.4724e+09	0.1919	3.3344
37	6.3529e+09	0.1744	3.2117
67	6.2910e+09	0.1653	3.2897
15347	6.3866e+09	0.1707	3.2093
25647	6.4637e+09	0.1806	3.3474
36489	6.3367e+09	0.1743	3.1773

results from the 9 simulations were recorded in terms of sorted maximum amplitudes and related probability values. The maximum amplitudes are taken from each up-crossing period, which is the maximum value of each up-crossing period. The probabilities were defined as:

$$P_X(x > X_i) = \frac{i}{N + 1} \tag{7.24}$$

where X_i: the i-th largest response amplitudes
i=1: largest
i=N: smallest
N: total number of amplitudes

The 40% largest wave amplitude from all maxima in terms of probability is presented in Figure 7.14. It can be seen that as the response amplitudes become higher, the difference between different seeds are more significant. The largest maxima in different seeds shows up to 30% difference. Thus it can be concluded that different seed values will give different extreme values. Which seed can provide an accurate result?
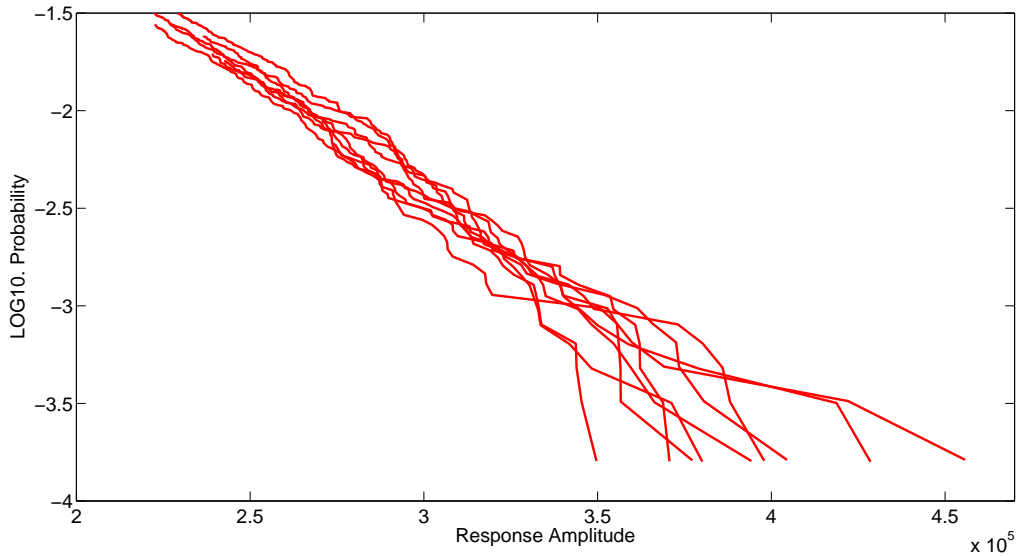
Figure 7.14: Comparison of Largest Samples from 9 Simulations of Riser Response With Different Seed Value. Use of Deterministic Amplitude and Stochastic Phase Angle

From Martin Fabrin Lagstad's master thesis *Response Estimation of Mooring Lines on the Floating Wind Turbine Hywind Demo*, it says that his supervisor Tor David Hanson from Statoil suggested small odd numbers, while Andreas Amundsen and Elizabeth Pazzano from MARINTEK suggested that the seeds should be large and odd numbers, but not larger than $2^{31} - 1$, and professor Carl Martin Larsen suggested large, odd numbers, preferably at least 5 digits.

Instead of choosing the seed that will provide the most accurate result, conference paper *Numerical Simulation for Installation of Offshore Wind Turbine Monopiles Using Floating Vessles* from Lin Li, Zhen Gao and Torgeir Moan use the result from 30 random seeds to obtain convergent results for the extreme responses. The result showed that 30 seeds were enough to obtain good convergent results. The result will be shown in the final discussion.

Simulation Length

Comparing with the result from Table 7.3, which is the 40-minute simulation for selecting design storm, we can see a significant deviation in skewness and kurtosis. For the same seastate $H_s = 7m$ and $T_p = 7.5s$ simulated with the same seed value, the variance, skewness and kurtosis obtained from different simulation lengths are shown in Table 7.6. However, since the 40-minute simulation is only for choosing design storm for maximum bending moment, plus the uncertainty existed equally in all seastates, it is acceptable. In addition, that is the reason that much longer simulations (8 hours) were performed, for reducing the statistical uncertainty.

Table 7.6: Comparison of variance, skewness and kurtosis value from different simulation length

Simulation Length	Variance	Skewness	Kurtosis
40 minutes	5.0920e+09	0.3995	4.0050
8 hours	6.3866e+09	0.1707	3.2093

Selection of Tail Function

As it was illustrated in last section *Distribution Fitting*, the number of data points selected to fit the three-weibull distribution will influence the lifetime extreme value. The selection of the extreme data on the tail of the distribution should give the least fitting error. From Table 7.4, it can be seen that the deviation between the selection of 434 and 306 data points on the tail was around 1%. In this thesis, only two cases were compared. It would give a more accurate result if more cases of different data points can be compared, and the one gives the least error can be selected to fit the Weibull distribution.

7.12   Results from SLST

In the three-parameter Weibull distribution, the lifetime extreme bending moment can be read out from the corresponding probability of exceedance. Different seed values can give different bending moment results because of the simulation uncertainty. The Mean value of different cases can be taken as the final result[22].

Table 7.7: Result from the SLTS method using three-parameter Weibull distribution

Seed	Above max% included	Above-[kN·m]	x50 [kN·m]	NO. of data points
1	47	177.32	357.3	549
3	47	185.29	365.5	503
7	47	173.23	348.1	605
13	47	178.66	381.1	560
37	48	164.35	356.4	674
67	46	187.03	357.4	494
15347	46	190.12	350.8	453
25647	45	201.42	362.0	408
36489	45	214.21	343.0	306
		Mean	358.0	

Chapter 8

Discussion

8.1 Rayleigh Distribution V.S. Weibull Distribution

As it is known that, Rayleigh distribution is not suitable to be used to describe nonlinear process. In order to illustrate the reason that the Rayleigh distribution does not fit the nonlineaer process more clearly, and how the Rayleigh distribution was replaced by Weibull distribution, response distribution fitting using both Rayleigh and Weibull distribution were compared.

Firstly, in order to plot Rayleigh cumulative distribution in the Weibull plot, it needs to be linearized by linearized variables. The Rayleigh distribution expressed by variance is given as:

$$F(x) = 1 - e^{-\frac{x^2}{2\sigma^2}} \tag{8.1}$$

The linearized equation of Rayleigh distribution is:

$$In(In(\frac{1}{1-F(x)}) = 2In(x) - In(2\sigma^2) \tag{8.2}$$

Thus the linearized variables can be obtained:

$$\tilde{y} = In(In(\frac{1}{1-F(x)})) \tag{8.3}$$

$$\tilde{x} = In(x) \tag{8.4}$$

Comparing with the linearized Weibull distribution, it is easy to find that two-parameter Weibull distribution and Rayleigh distribution have identical linearized variables. Figure 8.1 illustrates the Rayleigh distribution fitting and two-parameter Weibull for extreme value distribution. As it can be seen, Rayleigh distribution is totally out of range, it cannot fit the distribution all at. Neither two-parameter Weibull distribution was a good fitting. The biggest difference between these two fitting is Rayleigh distribution is a one-parameter distribution, it was decided by the variance from the extreme distribution. However, Weibull distribution can be two or three-parameter distribution, it can be adjusted to fit the distribution. Rayleigh distribution is fixed, it cannot be changed. Figure 8.1 illustrated the fitting to all maxima points. What happened if only the tail is fitted?
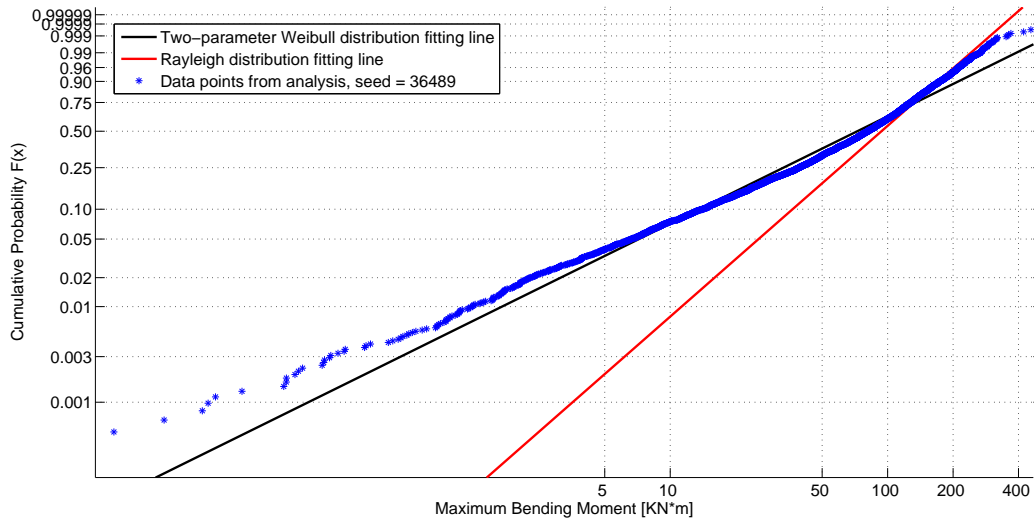
Figure 8.1: Distribution fitting using **two-parameter** Weibull distribution fitting and Rayleigh distribution fitting
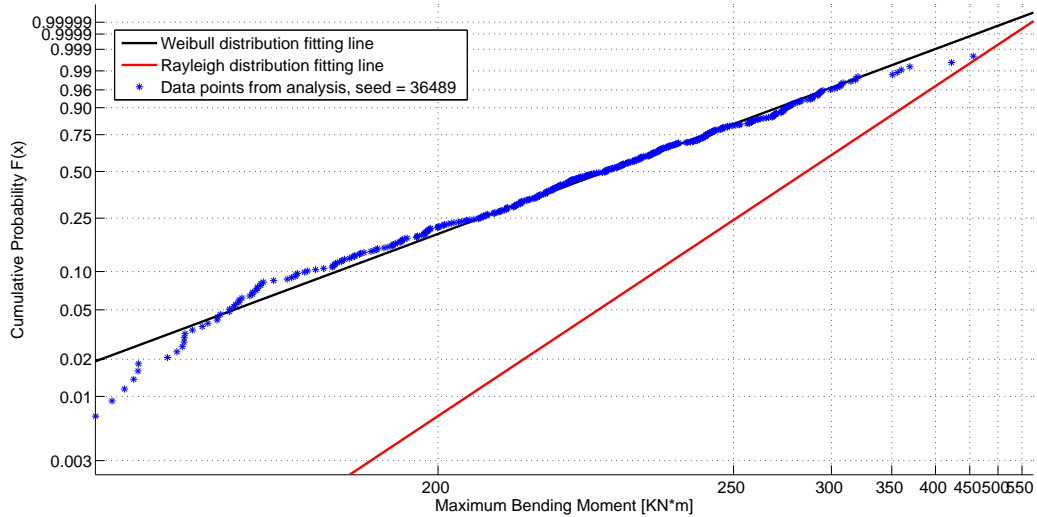

Figure 8.2: Distribution fitting using **three-parameter** Weibull distribution fitting and Rayleigh distribution fitting for 42% limit

Figure 8.2 shows the Rayleigh and three-parameter Weibull distribution fitting to 42% limit of the extreme distribution. A three-parameter Weibull distribution can give a satisfactory fitting by adding the location parameter, while Rayleigh distribution fitting was still out of range for the tail fitting. The Weibull distribution gives more flexibilities in fitting, thus it can be adjusted by its parameters. This is the reason why Rayleigh distribution cannot be used for this nonlinear process fitting.

8.2 Convergence Test of Maximum Bending Moment

As we can see from the results of maximum bending moment, the result from different seeds were different. In order to obtain reliable response, Lin Li[23] illustrated a convergence test for random seeds. In her paper, she compared the responses from 30 random seeds with the mean values of all 30 samples. Plus a cumulative averaged value for seed number i was also plotted to indicate the speed of convergence. The same procedure was applied to the result from SLTS method, to check whether the result can be converged.

Referred to Table 7.7, the convergence test for the maximum bending moment found in different seeds can be plotted in Figure 8.3. As we can see from 8.3, the results from
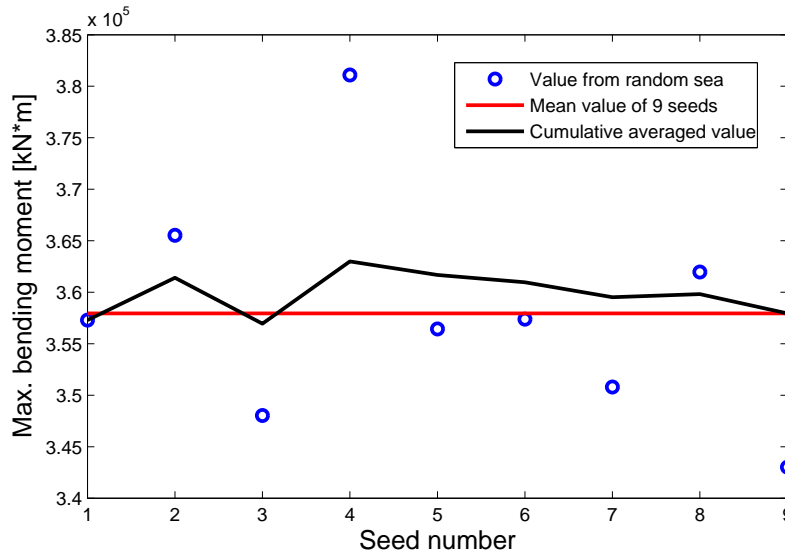
Figure 8.3: Convergence test results

9 seeds cannot fully converge, which means that the mean value is not reliable enough. The reason may be the samples are not big enough, more results from different seeds are needed. In Lin Li's[23] paper, 30 seeds were used. However, it is too time-consuming to perform more seed cases for this thesis. Another possible reason may be the number of data points selected to fit the three-parameter Weibull distribution was not the choice. As we can see from 7.7, only one limit percentage was tested. To make sure the distribution gives the least error, Equation 7.23 should be used to find the maximum limit percentage. In another word, since the three-parameter Weibull distribution was only applied to the tail of the nonlinear distribution. From which point it gives the best tail? That is the problem to be figured out. In this thesis, the Matlab code to find the best 'tail' which

gives the least error could not be finished. Thus only one max% was used for each seed. It can be a further work to perform more cases to prove that from how many seed cases a reliable result can be obtained, and codes to find the best max% for Weibull distribution fitting. These can be the methods to reduce the statistical uncertainty.

Chapter 9

Conclusion Remarks

9.1 Conclusion

The SLTS method has been used to estimate the lifetime extreme bending moment of a drilling tensioned riser in this thesis. The original SLTS method was based on long-term wave statistic, approximate long-term response statistic on frequency domain and short-term analysis on a design storm on time domain. The reason for approximate long-term wave statistic analysis is to limit the seastate number, hence the simulation time can be reduced. However, since there is no frequency solver in *SIMA*, the approximate long-term response statistic must be performed in time-domain. Since frequency solver is much faster than time domain solver, this would increase the total simulation time. The main purpose of time-domain analysis on this stage is to find a stable zero up-crossing period and variance to establish an approximate long-term response analysis, further on the design storm can be selected. The simulation length of design storm was chosen to be 8 hours, while the return period of the seastate is 3 hours. Some findings from this thesis are listed:

- In terms of extreme waves, selected seastates which give significant influence to the long-term distribution can represent the whole sea condition adequately. Wave amplitudes from selected seastates and all seastates showed neglected deviation.

- A 8-hour simulation was performed for one of the selected seastate in order to decide the time length that a stable variance can be obtained. The result showed that 40-minute simulation can achieve the goal.

- Deterministic amplitude and stochastic phase angle method was used to generate irregular wave. Result from the comparison of largest sample of 9 simulation of riser response with different seed values showed that, the deviation of largest bending moment amplitude can be up to 30%. Hence stochastic phase angle contributes an important uncertainty issue to the simulation.

- Approximate skewness and kurtosis were calculated for all selected seastates in approximate long-term distribution. The result of skewness varied from 0.15 - 0.40, kurtosis varied from 3.26 - 4.00 respectively. It means that the bending moment distribution has strong nonliear nature.

- Both two-parameter and three-parameter Weibull distribution were used to fit the extreme value distribution, neither could give an adequate fitting. The problem is

the linear part of the distribution was dominating the Weibull distribution. However the upper tail of the distribution was nonlinear and could not fit the Weibull distribution, which is the most interesting part in this thesis.

- The *Tail Function Approach* was introduced to represent the tail of the extreme value distribution. By fitting only the tail of the distribution, a three-parameter Weibull distribution could give a satisfactory outcome.

- Probability of exceedance of the lifetime extreme bending moment was estimated in long-term response distribution, which was calculated by Rayleigh distribution. This is a significant difference compared to environmental contour line method, that SLTS method can decide its own probability of exceedance.

- The lifetime extreme bending moment can be estimated for 9 different seed values. The result showed that the deviation of values from different seed was up to 11%. It was a significant uncertainty, to decide what is the final extreme value. An mean value is easy to access, but it may not give an adequate result. However, if a mean value is taken as the final result, results from more seed values can reduce the uncertainty. An convergence test can be established as an indicator, to decide whether a mean value can be the final result. A distribution maybe can be used to fit the results from different seed values, reading out the final result with an adequate probability of exceedance.

- The uncertainty of tail function approach was also studied. Two tail functions with 434 and 306 data points respectively were used to fit the three-parameter Weibull distribution, the deviation of the final result is around 1%. It is not a significant deviation compared to it from different seed values.

As we can see from the listed findings, SLTS method gives considerable uncertainties. The most significant one was from different seed values. A convergence test showed that 9 seeds are not enough to obtain a stable result. In order to find a more accurate extreme bending moment, more seeds should be simulated.

9.2 Further Work

In terms of this thesis, further work can be focused on the uncertainty of the simulation, such as the choice of seed values. Since the simulation length of each design storm is 8 hours, if less seed values can give an accurate result, if can significantly reduce simulation time. A suggestion is to use a proper distribution to fit the result from different seed values, and find the final result based on a probability of exceedance.

Appendix A

Matlab Code for Weibull Distribution

```matlab
%%%%%%%%%%%%%%%%%%%%%%%%%%%%%%%%%%%%%%%%%%%%%%%%%%%%%%%%%%%%%%%%%%%%%%%%%%%%%%%%%
% weibull3.m
%
% This is a Matlab file to calculate the 3 parameter Weibull cdf and it
% estimates the maximum force for the 50 year return period x50. It also
% plots the data, the estimation and a weibull fitting line.
%
% Note: The user must provide the correct path
%
% INPUT
%  moment time history data .txt from SIMA
%
% OUTPUT
%  The estimated maximum force for a 50 year return period x50
%
% Author: Xiao Gan, June 2013
%%%%%%%%%%%%%%%%%%%%%%%%%%%%%%%%%%%%%%%%%%%%%%%%%%%%%%%%%%%%%%%%%%%%%%%%%%%%%%%%%
%% Reading data from files
    clc
    clear all
%    str = ['result/all_seastates/',num2str(j),'.txt'];
    dlmread('result/tp7.5/9.txt');
    prob_per = 0; % n% of the maxima
    t=ans; % getting time history data from SIMA output file
    Le = length(t(:,2)); % steps of the time history data
    a = t(801:Le,1:2);
    L = length(a(:,1)); % steps of the time history data without the first 200
        seconds
    prob_per = 0; % n% of the maxima
%% Location parameter
        x0=0; % Location parameter seed_9 two parameter weibull
%% Calculating zero upcrossing period
  temp = [];
    for i = 1:(L-1)
        if a(i,2)<0 && a(i+1,2)>0
```

```matlab
        temp = [temp,a(i,1)];
        end
    end
    c = temp; % zero upcrossing time
%% Calculating individual maxima
m = zeros(length(c)-1,1);
temp = [];
for i = 1:(length(c)-1)
    for j = round((c(i)-200)*4):round((c(i+1)-200)*4)
    temp = [temp,a(j,2)];
    end
    m(i,1) = max(temp); % Extreme value in every zero upcrossing period
    temp = [];
end
Max = sort(m); %sorting the found maximas
prob = zeros(length(c)-1,1);
for i=1:(length(c)-1)
    prob(i,1)=i/(1+length(c)); % calculating probability for all maxima points
end
%% Selecting n% maxima
temp = [];
for i=1:length(Max) % Selecting n% maxima
    if Max(i,1) > (prob_per*Max(length(Max),1))
        temp = [temp,Max(i,1)];
    end
end
Maxp = temp;     % n% maxima
inverse_maxp= zeros ( length(Maxp),1);
for i=1:length(Maxp)
    inverse_maxp(i,1)=Maxp(1,i);
end
F = zeros(length(Maxp),1); % Cumulative probability of the n% maxima sample
for i=1:1:length(Maxp)
    F(i,1)=i/(length(Maxp)+1);
end
%% Lineared variables
Y = log(-log(1-F));      % Linearized Y axis of n% maxima for Weibull dist.
% Y = log(-log(1-prob)); % Linearized Y axis of all maxima for Weibull dist.
X=zeros(length(Maxp),1); % Linearized X axis of n% maxima for Weibull dist.
  for j = 1:length(Maxp)
    X(j,1)=log(Maxp(1,j)-x0);
  end
% X=zeros(length(Max),1); % Linearized X axis of all maxima for Weibull dist.
%   for j = 1:length(Max)
%       X(j,1)=log(Max(j,1)-x0);
%   end
%% Plotting fitted straight line for weibull distribution
[fitobject,gof,output] = fit(X,Y,'poly1');
lamda_1 = fitobject.p1;
lamda_2 = fitobject.p2;
c = (1:1.1*max(X));
```

```matlab
plot(c*lamda_1+lamda_2,'k','LineWidth',2); % Weibull fitted line
hold on
plot(X(:,1),Y,'*') % Original data points
hold on
% axis([X(2,1) 1.01*max(X) min(Y) log(-log(0.0001))]); % For 3-parameter
    Weibull
axis([X(2,1) 1.004*max(X) min(Y) log(-log(0.000001))]); % For 2-parameter
    Weibull
%% Plotting largest expected moment
%0.999971 is the probability level for the 50 year response. 1-Q=0.999971,
%found in Iteration.m
% It should be scale according to the number of maxima used in the tail
% function
prob_exceedance = 0.999971;
%prob_exceed_scale = prob_exceedance/(L-length(Maxp))*L; % The probability of
    exceedance must be scaled! since only part of the data was considered
prob_exceed_scale=((prob_exceedance*(L+1))-(L-length(Maxp)))/(1+length(Maxp));
    % The probability of exceedance must be scaled! since only part of the
    data was considered
plotprobmax=log(-log(1-prob_exceed_scale));
%Plotting the x50, the largest expected bending moment [kN] in 50 years
x50 = (plotprobmax-lamda_2)/lamda_1;
plot(x50,plotprobmax,'ro','LineWidth',2);
hold on
line([X(1,1),x50],[plotprobmax,plotprobmax],'color','r','LineWidth',2);
line([x50,x50],[min(Y),plotprobmax],'color','r','LineWidth',2);
% line([max(X),max(X)],[min(Y),plotprobmax],'color','r'); % For 2-parameter
x50_bending = exp(x50)+x0; % maximum bending moment
%% Making a Weibull plot; loglog vs log
p     = [0.001 0.003 0.01 0.02 0.05 0.10 0.25 0.5...
        0.75 0.90 0.96 0.99 0.999 0.9999];

label = {'0.001','0.003', '0.01','0.02','0.05','0.10','0.25','0.50', ...
        '0.75','0.90','0.96','0.99', '0.999','0.9999'};

tick = log(log(1./(1-p)));
set(gca,'YTick',tick,'YTickLabel',label,'XScale','lin'); % Ytick: store the
    location of the Ytick marks; YtickLable: lable the tick marks

tick = [5 10 50 100 200 400]; % For 2-parameter; Bending moment shown in axis
    note: unit is KN
% tick = [200 250 300 350 400];
xtick = log(1000*tick-x0);
XTickLabel=cell(length(xtick),1);
for i=1:length(xtick),
XTickLabel{i}=sprintf('%.0f ', tick(i));
end
set(gca, 'XTick', xtick, 'XTickLabel', XTickLabel);
% rotateticklabel(gca,45);
% xticklabel_rotate(xtick,90,XTickLabel)
```

```matlab
xlabel('Maximum Bending Moment [KN*m]','FontSize',14);
ylabel('Cumulative Probability F(x)','FontSize',14);
% title('3-Parameter Weibull Probability Plot');
legend('Weibull distribution fitting line','Data points from analysis, seed =
    36489','Probability of exceedance');
set(gca,'FontSize',14)
box off
grid on
```

```matlab
xlabel('Maximum Bending Moment [KN*m]','FontSize',14);
ylabel('Cumulative Probability F(x)','FontSize',14);
```

Appendix B

Weibull Distribution Fitting for All Seeds
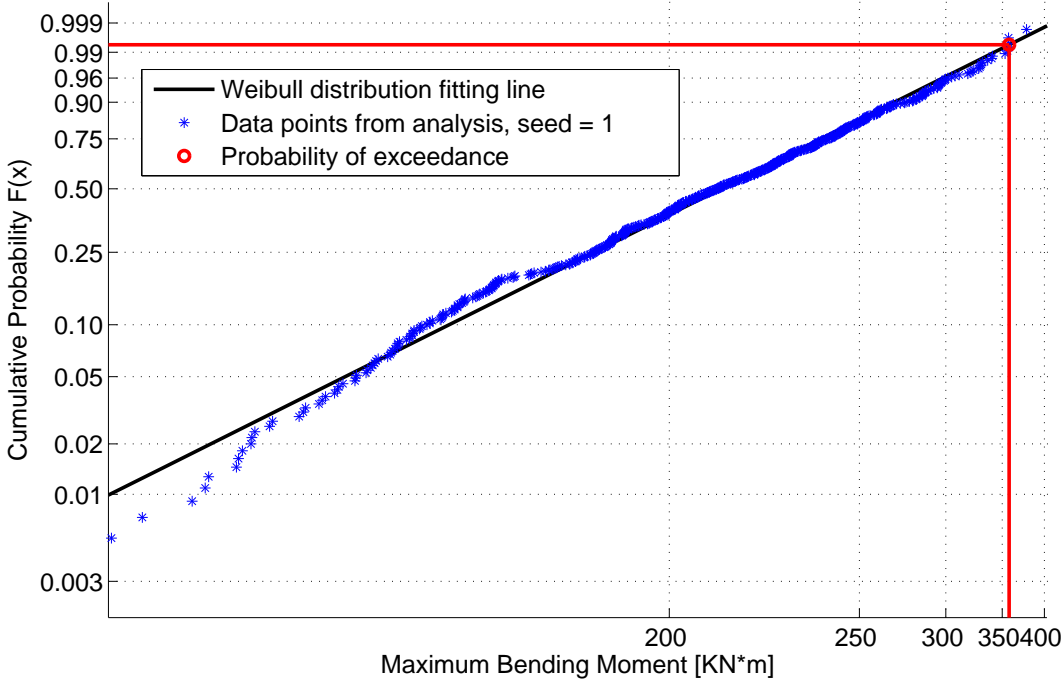
Figure B.1: Distribution fitting using three-parameter Weibull distribution for seed=1
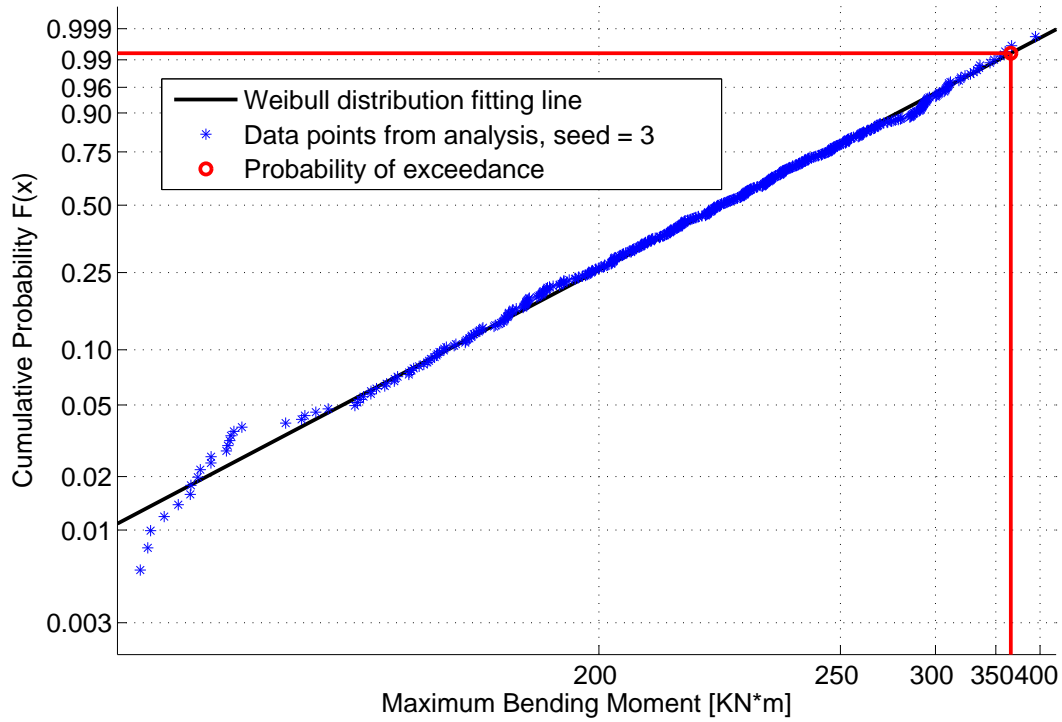
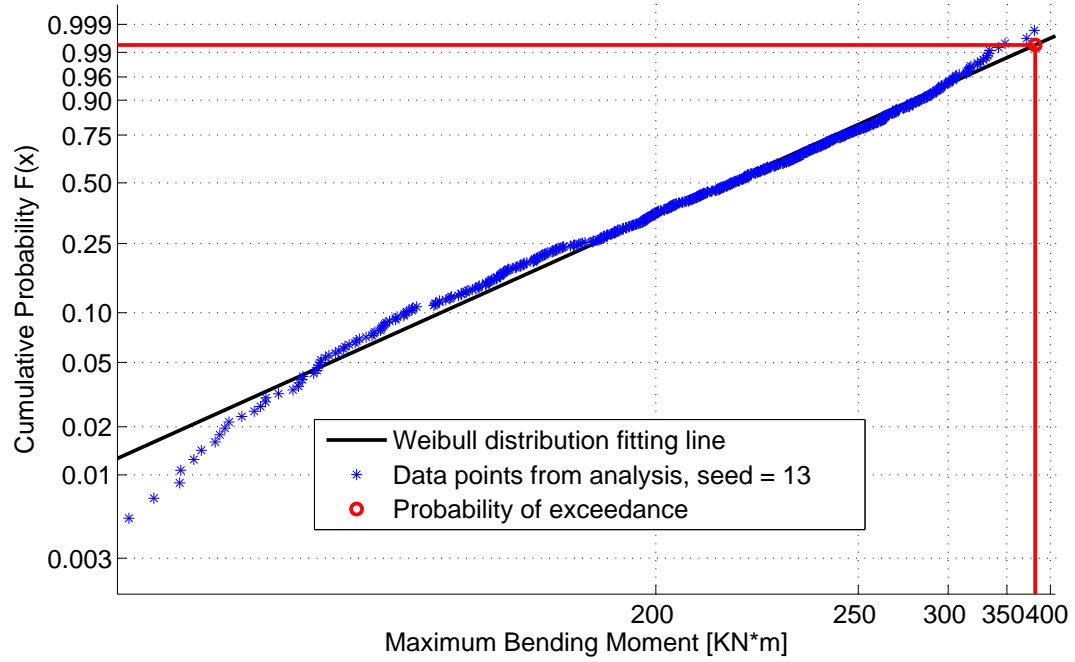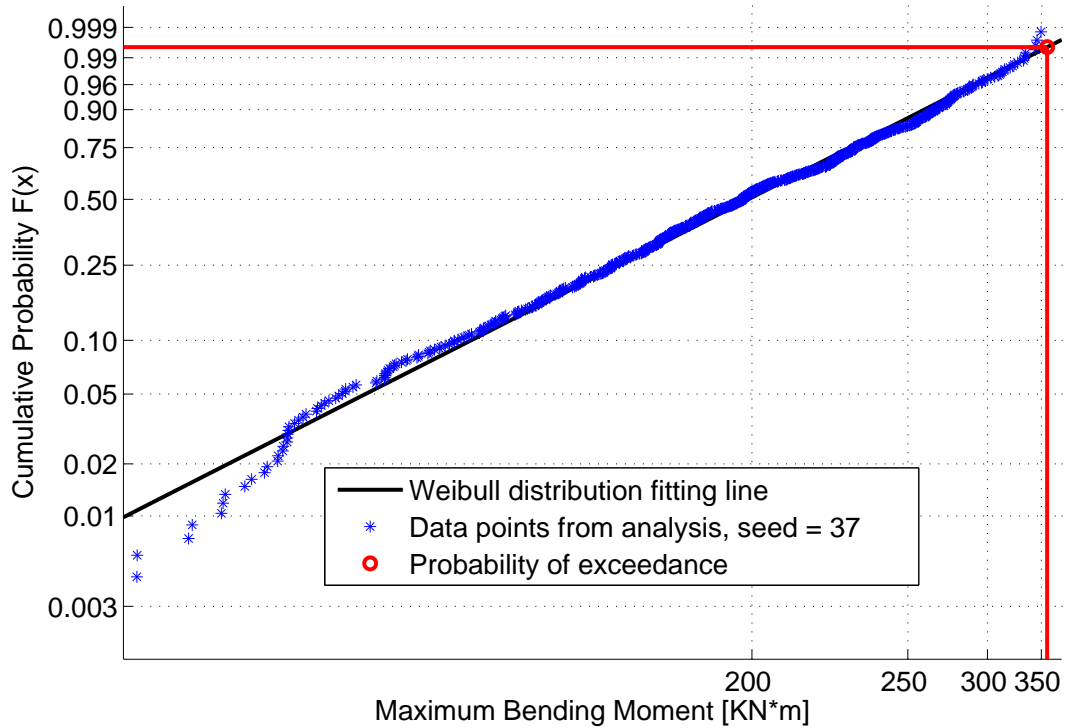**Figure B.2:** Distribution fitting using three-parameter Weibull distribution for seed=3
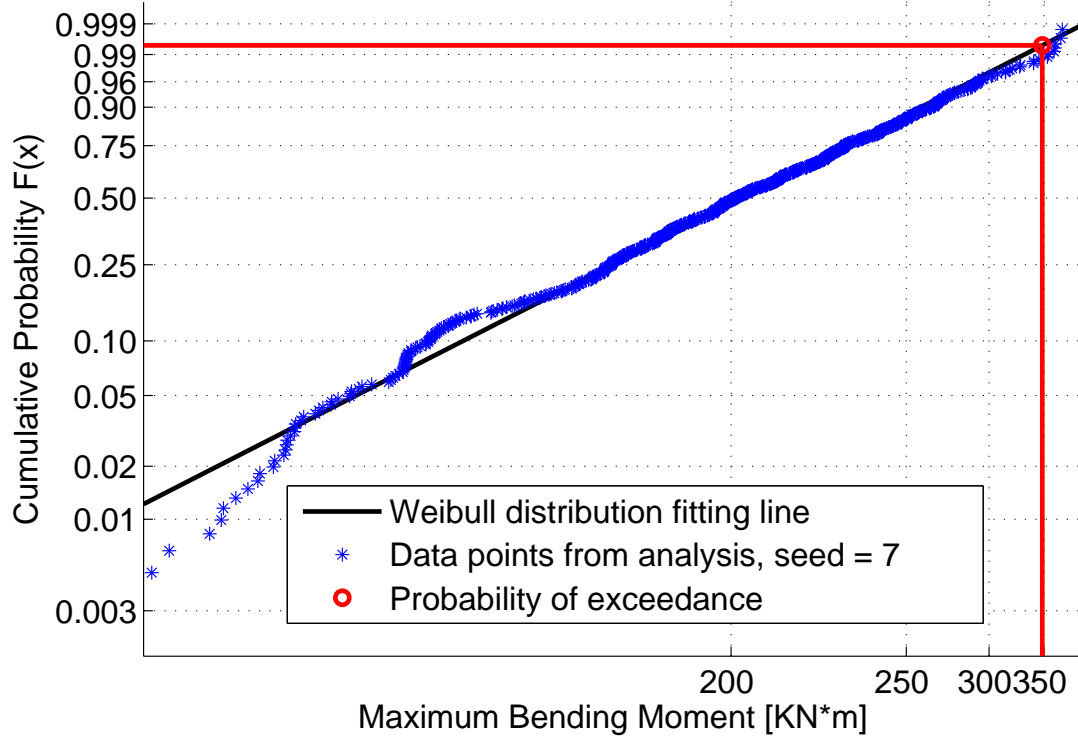
Figure B.3: Distribution fitting using three-parameter Weibull distribution for seed=7

Figure B.4: Distribution fitting using three-parameter Weibull distribution for seed=13

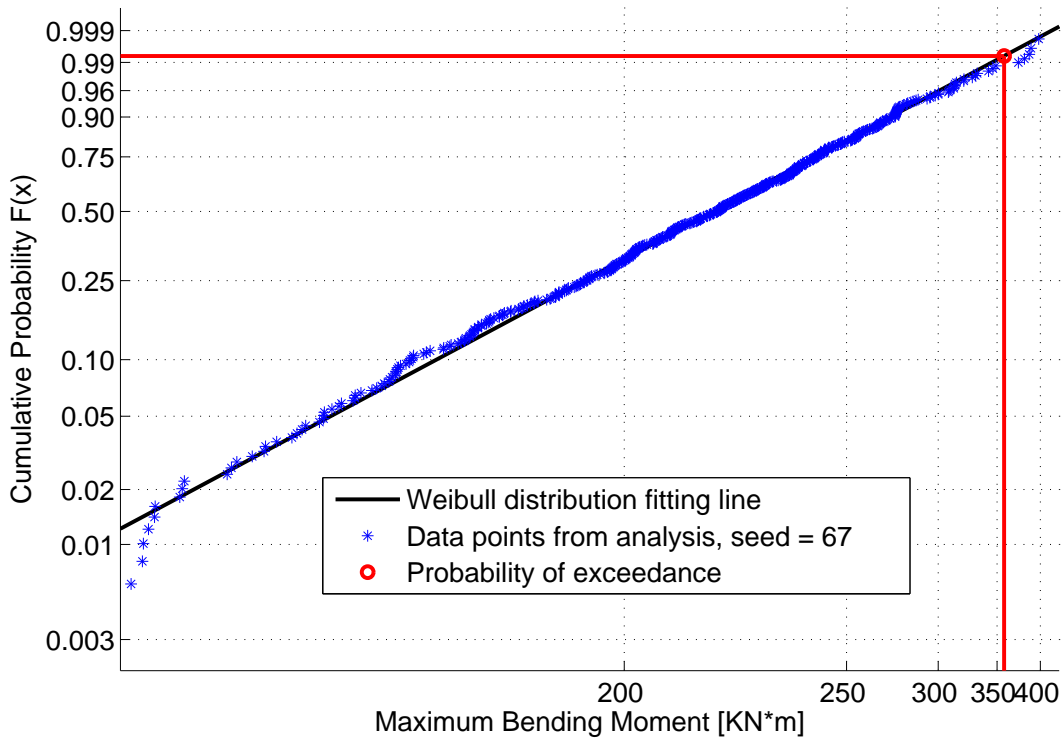**Figure B.5:** Distribution fitting using three-parameter Weibull distribution for seed=37

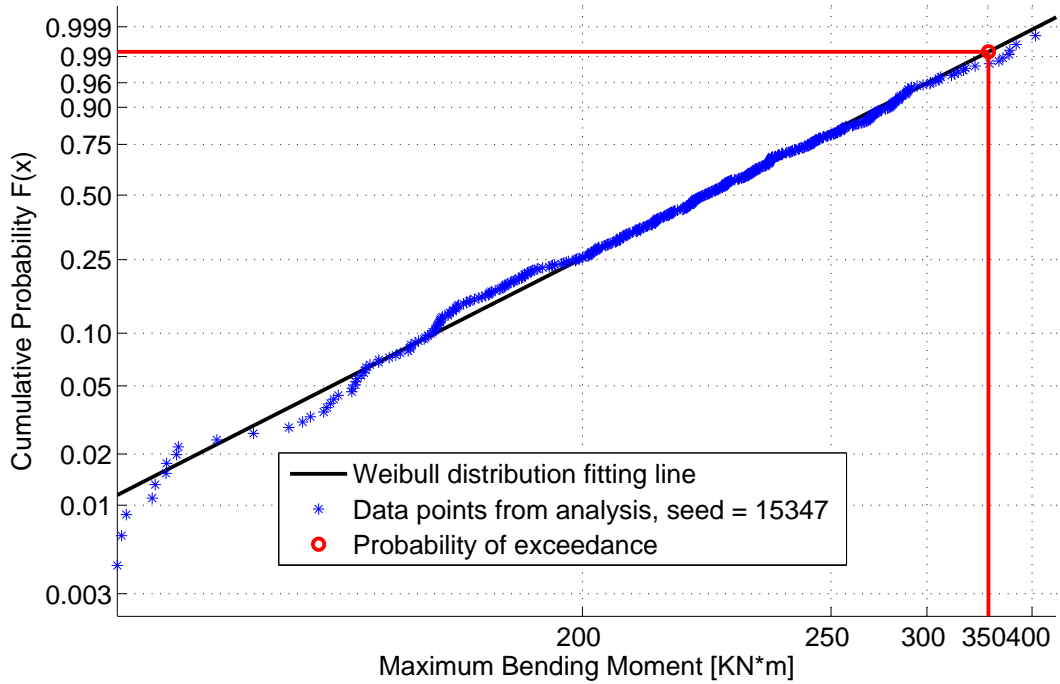**Figure B.6:** Distribution fitting using three-parameter Weibull distribution for seed=67
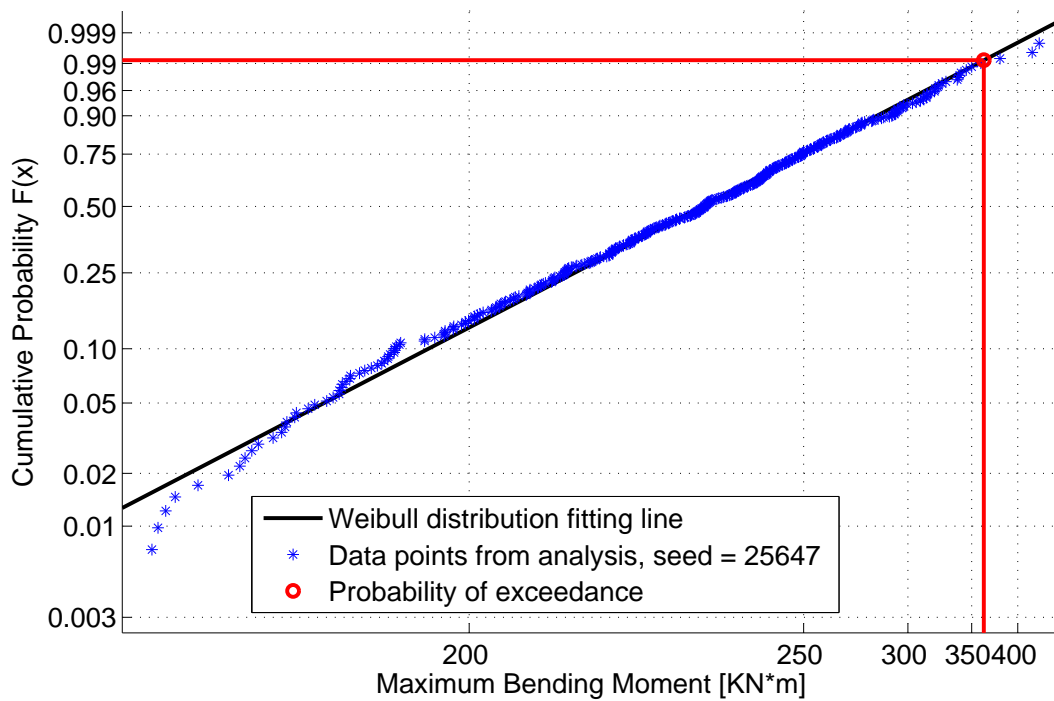

Figure B.7: Distribution fitting using three-parameter Weibull distribution for seed=15347

Figure B.8: Distribution fitting using three-parameter Weibull distribution for seed=25647

Bibliography

[1] Yong Bai and Qiang Bai. *Subsea Engineering Handbook*. Elsevier, 2010.

[2] "drilling riser". Wikipedia. `http://en.wikipedia.org/wiki/Drilling_riser`, cited February 2014.

[3] C. P. Sparks. *Fundamental of Marine Riser Mechanics*. Pennwell publishing company, 2007.

[4] Ronny Sten, Michael Rygaard Hansen, Carl Martin Larsen, and Svein Savik. Force variations on heave compensating system for ultra-deepwater drilling risers. In *OMAE2010-20011*, 2010.

[5] *Compendium for couse Marine Dynamics, Irregular Wave*. Department of Marine Technology, Norwegian University of Science and Technology.

[6] *USFOS Hydrodynamics, Theory Description of Use Verification*.

[7] Harald Ormberg and Elizabeth Passano. *RIFLEX User's Manual*. Norwegian Marine Technology Research Institute, 2013.

[8] Det Norske Veritas. *Environmental Conditions and Environmental Loads*, October 2010.

[9] Laboratory of Scientific Computing and Visualization, Federal Universiy of Alagoas. *On the Assessment of Extreme Response of Steel Risers*, Maceio, Alagoas, Brazil, 2009.

[10] Carl Martin Larsen and Elizabeth Passano. Extreme response estimation for marine risers. In *OMAE1990*, 1990.

[11] Morten Reve. Understanding of buoyancy in drill pipe and risers. Master's thesis, University of Stavanger, 2013.

[12] Ronny Sten. *Dynamic Simulation of Deep Water Drilling Risers with Heave Compensation System*. PhD thesis, Norwegian University of Science and Technology, 2012.

[13] Harald Ormberg and Elizabeth Passano. *RIFLEX Theory Manual*. Norwegian Marine Technology Research Institute, 2012.

[14] Haver S. *Prediction of Characteristic Response*. Statoil ASA Internal, 2011.

[15] M. J. Tucker, P. G. Challeror, and D. J. T. Carter. Numerical simulation of a random sea: a common error and its effect upon wave group statistics. *Applied Ocean Research*, 6(2), 1984.

[16] Elizabeth Passano. *Efficient Analysis of Nonlinear Slender Marine Structures*. PhD thesis, The Norwegian Institute of Technology, 1994.

[17] Arvid Naess and Torgeir Moan. *Stochastic Dynamics of Marine Structures*. Cambridge University Press, 2013.

[18] S. Haver and S.R. Winterstein. Environmental contour lines: A method for estimating long term extremes by a short term analysis. 2008.

[19] A.D. Trim. Time-domain random dynamic analysis of marine risers and estimation of non-gaussian bending stress statistics. *Applied Ocean Research*, 12(4), 1990.

[20] ReliaSoft Corporation. Reliasoft. `http://http://www.reliasoft.com/`, cited June 2014.

[21] *Compendium for couse Stochastic Theory of Sealoads*. Department of Marine Technology, Norwegian University of Science and Technology.

[22] Nils Rune Sodahl. *Methods for Design and Analysis of Flexible Risers*. PhD thesis, The Norwegian Institute of Technology, 1991.

[23] Lin Li, Zhen Gao, and Torgeir Moan. Numerical simulation for installation of offshore wind turbine monopiles using floating vessles. In *OMAE2013*, 2013.